

4. SITE 810¹

Shipboard Scientific Party²

Hole 810A

Date occupied: 22 July 1990
Date departed: 22 July 1990
Time on hole: 8 hr 15 min
Position: 32°25.37'N, 157°50.75'E
Bottom felt (rig floor; m; drill pipe measurement): 2633.0
Distance between rig floor and sea level (m): 11.1
Water depth (drill pipe measurement from sea level, m): 2621.9
Total depth (rig floor; m): 2642.5
Penetration (m): 9.50
Number of cores (including cores with no recovery): 1
Total length of cored section (m): 9.50
Total core recovered (m): 9.74
Core recovery (%): 102
Oldest sediment cored:
Depth sub-bottom (m): 9.74
Nature: nannofossil ooze
Earliest age: late Pleistocene
Measured velocity (km/s): n/a
Note: a single core was taken for ODP geriatric studies.

Hole 810B

Date occupied: 22 July 1990
Date departed: 22 July 1990
Time on hole: 2 hr, 30 min
Position: 37°25.37'N, 157°50.75'E
Bottom felt (rig floor; m; drill pipe measurement): 2633.0
Distance between rig floor and sea level (m): 11.1
Water depth (drill pipe measurement from sea level, m): 2621.9
Total depth (rig floor; m): 2693.0
Penetration (m): 60.00
Number of cores (including cores with no recovery): 0
Total length of cored section (m): 0.00
Total core recovered (m): 0.00
Core recovery (%): 0
Note: Wash-in test to establish length of drill-in conductor casing.

Hole 810C

Date occupied: 22 July 1990
Date departed: 22 July 1990
Time on hole: 19 hr, 15 min
Position: 32°25.40'N, 157°50.74'E
Bottom felt (rig floor; m; drill pipe measurement): 2634.1
Distance between rig floor and sea level (m): 11.1
Water depth (drill pipe measurement from sea level, m): 2623.0
Total depth (rig floor; m): 2770.2
Penetration (m): 136.10
Number of cores (including cores with no recovery): 16
Total length of cored section (m): 136.10
Total core recovered (m): 143.81
Core recovery (%): 105
Oldest sediment cored:
Depth sub-bottom (m): 136.10
Nature: nannofossil ooze and chert
Earliest age:
Latest age: early Maestrichtian
Measured velocity (km/s): 1.62 (ooze); 1.66 (chert)

Hole 810D

Date occupied: 23 July 1990
Date departed: 29 July 1990
Time on hole: 6 days, 2 hr, 30 min
Position: 32°25.36'N, 157°50.73'E
Bottom felt (rig floor; m; drill pipe measurement): 2534.1
Distance between rig floor and sea level (m): 11.1
Water depth (drill pipe measurement from sea level, m): 2623.0
Total depth (rig floor; m):
Penetration (m): 0.00
Number of cores (including cores with no recovery): 0
Total length of cored section (m): 0.00
Total core recovered (m): 0.00
Core recovery (%): 0
Note: A reentry cone was placed over this hole, but no casing was successfully suspended from it, and no hole was cored.

SITE SUMMARY

The principal objective of Site 810 was to drill interbedded cherts and chalks of Mesozoic age on Shatsky Rise using the diamond-coring system (DCS). This objective was not achieved because of difficulties in setting up a reentry cone on the seafloor,

¹ Storms, M. A., Natland, J. H., et al., 1991. *Proc. ODP, Init. Repts.*, 132: College Station, TX (Ocean Drilling Program).

² Shipboard Scientific Party is as given in the list of participants preceding the contents.

shortage of time toward the end of the leg, and approaching typhoons, which made operations on the suspended DCS platform in the derrick too dangerous to begin. We did manage to core a shortened section of Cretaceous (Maestrichtian)-Cenozoic nanofossil oozes with the advanced piston corer (APC), and attempted to set up the reentry cone, before abandoning the site.

Approach to Site and Coring Operations

Shatsky Rise was approached from the southwest, and the ship passed over previously drilled DSDP Sites 306 and 305 in that order at 8 kt, to link them to Site 810 with a continuous seismic reflection profile. Steaming from south to north, we traced the principal chert horizon seismically to a point where the pelagic sediments capping it are only 0.07 s thick, and dropped the beacon at 0600 hr on 22 July 1990. In order, we then recovered a single APC core for geriatric studies in Hole 810A, did a wash-in test to a sub-bottom depth of 60 m in Hole 810B to determine the length of conductor casing needed below the reentry cone, and continuously piston-cored from a precisely located mud line to the uppermost substantial chert horizon at 125 m below the seafloor (mbsf) in Hole 810C. One additional core was taken with the extended core barrel (XCB) in Hole 810C before we retrieved the drill pipe and lowered the reentry cone.

Attempts to Emplace a Reentry Cone

The principal difficulties with the reentry cone installation at Hole 810D had to do with suspending casing in the casing hanger. Even before the reentry cone was lowered, one casing string was inadvertently dropped from the moon pool to the seafloor, evidently having become unthreaded while attempting to land the casing hanger. The hanger was removed and modified, but then became wedged in the cone on a test and could not be removed. This meant that no casing could be suspended from it. We decided to lower the cone as it was, but added 14 drums of pig-iron ingots, plentifully available on board ship, to the skirt at the base of the cone, in order to replace the weight the casing would have provided the assembly on the seafloor. This weight was required to tension the drill string properly during anticipated DCS coring operations.

After this cone was landed on the seafloor, we experienced repeated difficulties in trying to seat a drill-in bottom-hole assembly (DI-BHA). At first, it appeared that the back-off nut was not operating properly, but when the drill string was retrieved to inspect it, we found that the mechanism had landed properly, but concluded that the key-slots which prevent the DI-BHA from unscrewing had failed, thus preventing back-off. We lowered the DI-BHA again, this time without tightening the back-off nut so that with only a small amount of frictional resistance it would back off. But once again, the mechanism did not work, and the DI-BHA became stuck. After we freed it and retrieved the drill string, we found that a proper landing again had occurred, but that the back-off nut had fused or jammed into its landing shoulder, possibly by means of the frictional heat produced by rotation, or loads imposed in varied seating attempts. This inadvertent "weld" managed to hold the entire 45,000-lb DI-BHA on its trip back to the ship.

We made one final attempt to land the DI-BHA, this time with a new beveled C-ring in the landing assembly. However, the bevel proved to be our undoing, since the landing shoulder was too narrow, and simply compressed the C-ring on the bevel, allowing the entire DI-BHA to slip through the cone and drop into the soft ooze below. However, this appeared on deck to be a proper landing of the DI-BHA. The problem was only discovered when we could not get a sinker bar to the anticipated bottom of the DI-BHA in order to recover the center bit. When the drill string was retrieved, the back-off nut again was found to be fused or

wedged into the landing sleeve. Back-off had actually occurred, but this time the entire DI-BHA had fallen out of the cone.

Rig-down, Fishing the DI-BHA, and Subsequent Survey

With this reversal, there was no time left for DCS coring. With the approach of inclement weather, the DCS tubing was taken from its vertical rack in the derrick and laid out in joints for storage on the riser hatch. There was still sufficient time to attempt to fish the DI-BHA. This was accomplished, and all drill collars were on deck by late afternoon on 29 July 1990. All additional DCS hardware was then secured.

Since weather reports indicated that we still had as much as a day left before our departure would be mandatory, we proceeded to carry out a seismic survey of a portion of the summit of Shatsky Rise. We cut the survey somewhat short at noon on 31 July, when the ship's low barometer reading persuaded the Captain that we should leave the area with all possible speed.

Science Summary

At Site 810, Holes 810A and 810C, we recovered 129.8 m of Cenozoic and Upper Cretaceous nanofossil ooze. Table 1 gives the coring summary. The shortened section records hiatuses in the upper Miocene-lower Eocene, lower Eocene-upper/lower Paleocene, and lower Paleocene-upper Maestrichtian. A complete Cretaceous/Tertiary boundary was not present. The hiatuses represent intervals of erosion and redeposition in this shortened section. Many of the sediments contain reworked foraminiferal assemblages and show structural evidence for the action of currents. Five units are distinguished as follows:

Unit I (0-4.2 mbsf). Pleistocene brown to dark gray nanofossil ooze with cut-and-fill structures, and evidence for mixing of cooler- and warmer-water faunas.

Unit II (4.2-76.0 mbsf). Lower Pliocene to Pleistocene light gray to white nanofossil ooze, characterized by evidence for increasing dissolution and mixing downsection. The unit contains a number of thin and one quite thick (14 cm) ash beds and rounded pumiceous dropstones, derived from arc systems to the west.

Unit III (76.0-99.5 mbsf). Upper(?) Miocene to lower Pliocene pale tan to tan clayey nanofossil ooze and calcareous clay, with rhythmic color alternations corresponding to varying clay contents (highest estimated 70%). Foraminiferal assemblages

Table 1. Coring summary for Site 810.

Core	Date (July 1990)	Time	Depth (mbsf)	Cored (m)	Recovered (m)	Recovery (%)
1321-810A-1H	22	0445	0.0-9.5	9.5	9.74	102.0
Totals				9.5	9.74	102.0
132-810C-						
1H	22	0815	0.0-2.4	2.4	2.40	100.0
2H	22	0900	2.4-11.9	9.5	9.84	103.0
3H	22	0930	11.9-21.4	9.5	9.89	104.0
4H	22	1015	21.4-30.9	9.5	9.89	104.0
5H	22	1045	30.9-40.4	9.5	9.86	104.0
6H	22	1115	40.4-49.9	9.5	9.90	104.0
7H	22	1200	49.9-59.4	9.5	9.92	104.0
8H	22	1230	59.4-68.9	9.5	10.06	105.9
9H	22	1315	68.9-78.4	9.5	9.83	103.0
10H	22	1340	78.4-87.9	9.5	9.98	105.0
11H	22	1430	87.9-97.4	9.5	10.05	105.8
12H	22	1540	97.4-106.9	9.5	9.74	102.0
13H	22	1625	106.9-116.4	9.5	9.78	103.0
14H	22	1705	116.4-125.9	9.5	9.89	104.0
15H	22	1755	125.9-127.1	1.2	9.86	821.0
16X	22	1950	127.1-136.1	9.0	2.92	32.4
Totals				136.1	143.81	105.7

show evidence for strong dissolution. The base of the unit is at a hiatus.

Unit IV (99.5–113.3 mbsf). Upper Paleocene and lower Eocene pale tan nannofossil ooze, separated by a hiatus. Paleocene foraminiferal assemblages are strongly reworked, and include some Cretaceous forms. There is evidence for slumping and size sorting.

Unit V (113.3–136.1 mbsf). Upper Cretaceous to upper Paleocene white nannofossil ooze with large coccolith plates and small chert nodules. The pale color and coring deformation in the lower 10 m makes identification of structures difficult, but there is a hiatus across the Cretaceous/Tertiary boundary.

We obtained an excellent array of measurements for physical properties and magnetic susceptibility, which show strong correlations with cyclical lithological variations in the sediments. Although the section is broken by hiatuses, the upper two units carry detailed information relating to the development of eolian transport from the Asian mainland during the climatic deterioration that occurred between the Pliocene and Pleistocene.

BACKGROUND AND OBJECTIVES

Site 810 on Shatsky Rise was intended to test the capability of the DCS in recovering alternating very hard, flinty chert, and very soft calcareous chalk and ooze. The site was also to be the first deployment of a reentry cone modified for DCS coring. Whereas at Site 809, the hard rock base (HRB) provided the weight against which the drill string was held in tension, here the skin friction of the sediments against a DI-BHA plus the weight of that assembly was to provide much of the countering force.

Scientifically, the principal objective was recovery of soft calcareous material, and possibly black shales rich in organic carbon, between chert layers in Mesozoic sequences on Shatsky Rise. Shatsky Rise was selected for this test because it epitomizes the poor recovery of such material throughout the Pacific using rotary coring (Fischer, Heezen, et al., 1971; Larson, Moberly, et al., 1975). The black shales are particularly important to sample because of the possibility of synchronous anoxia in all the oceans at certain times during the Cretaceous (e.g., Schlanger and Jenkyns, 1976).

In order to determine the skin-friction parameters for the DI-BHA at Site 810, a preliminary hole was cored to a depth of 135 mbsf using the APC. This provided a section through a considerably shortened portion of the pelagic sediment cap that drapes Shatsky Rise. The section provides useful information concerning post-Cretaceous oceanographic conditions in this part of the Pacific, local conditions of sedimentation, erosion, and redeposition on Shatsky Rise, and the development of eolian transport since the Miocene. In addition, a single "mud-line" piston core from a separate hole was provided to the Ocean Drilling Program for a geriatric study.

The APC cores proved to be the only materials obtained at Site 810 because of a combination of operational difficulties in setting up the reentry cone, deteriorating weather conditions, and lack of time toward the end of the leg. The DCS was not used at this site.

OPERATIONS

Approach to Site

We approached Shatsky Rise on 21 July 1990 on a course of 094° at 8 kt, beginning seismic coverage just prior to passing over DSDP Site 306 on the south side of the Rise (Fig. 1). We changed course to 000° to pass over Site 305, tracing basement and chert horizons beneath a pelagic sediment cap thickening to the north (Fig. 1). We nearly paralleled a *Kana Keoki* profiler record on this course (Fig. 2) which showed that the pelagic cap first thickens

and then thins to a point where the upper "chert reflector" can be reached with only 150 m of drilling.

Although GPS navigation indicated that we were adhering closely to *Kana Keoki's* track, when we actually passed over the preliminary target (ENG-6 in Fig. 2), the pelagic cap proved to be considerably thicker than anticipated (about 250 m). This was more than we had time to drill and case off in an abbreviated program at this site. Evidently, the actual *Kana Keoki* track, which was navigated by satellite in 1977, was obtained in slightly deeper water somewhat west of our incoming track which was navigated by GPS.

We elected to continue north on the anticipation that the pelagic cap would thin still more, following an uppermost "chert reflector" using the 3.5 kHz echo sounder until the overlying sediments were only 0.07 s thick. This occurred beneath a flat area between possible channel structures in the pelagic cap (Fig. 3). Here, we dropped the beacon for Site 810 at 0600 hr on 22 July 1990. In the 3.5 kHz record, the "chert" reflector is actually a doublet, with the top reflector at about 115 mbsf and the lower one at about 125 mbsf, computed using a sediment velocity of 1.5 km/s (cf. Shatsky Rise, Site 577 chapter in Heath, Burckle, et al., 1985).

Site 810 Operations

Prior to setting a modified reentry cone at Site 810, three holes were spudded. One (Hole 810A) was to recover a mud-line piston core for an ongoing ODP geriatric core study. The second (Hole 810B) was a jet-in test to provide information required for washing in the 16 in. diameter casing (conductor pipe) to be attached to the bottom of the reentry cone. A third hole was cored using the ODP APC and XCB coring systems. This hole was necessary to locate the uppermost chert horizon in the section, and also to provide physical properties data on the calcareous ooze overlying the chert. These data were to be used in accessing what magnitude of skin friction could be expected against the casing and DI-BHA assemblies. This in turn would help to determine what degree of tensioning could ultimately be used with the tensioning jay-tool and tapered stress joint assemblies.

Hole 810A

Hole 810A was spudded at 1400 hr with the APC coring assembly. When recovered, the core barrel was filled with 9.74 m of calcareous ooze, with oxidized mud-line sediment at the top. Since this core was to be donated to the ODP geriatric core study, we did not re-spud the hole for a more accurate mud-line measurement. The bit cleared the mud line at 1415 hr ending Hole 810A.

Hole 810B

Hole 810B was a simple jet-in test to verify that an adequate amount of 16-in. casing could be washed in to tension the modified reentry cone. We decided to do the jet test prior to piston coring the section because of the potential risk in contacting a chert horizon with the APC. Such an impact might bend a core barrel, necessitating a pipe round-trip. A few minutes were taken to monitor pump pressure vs. flow rate prior to initiating the jetting procedure. An XCB core barrel with a center bit was dropped and at 1545 hr on 22 July 1990, Hole 810B was spudded. For jetting purposes the mud line was assumed to be at approximately 2633 m from the dual-elevator stool (DES) at the rig floor. The bit was washed to 2693 m or 60 mbsf at gradually increasing flow rates from 20 to 77 strokes-per-minute. No rotation was used but up to 10,000 lb weight-on-bit was ultimately required. Hole 810B was terminated at 1645 hr on 22 July 1990 when the bit cleared the mud line.

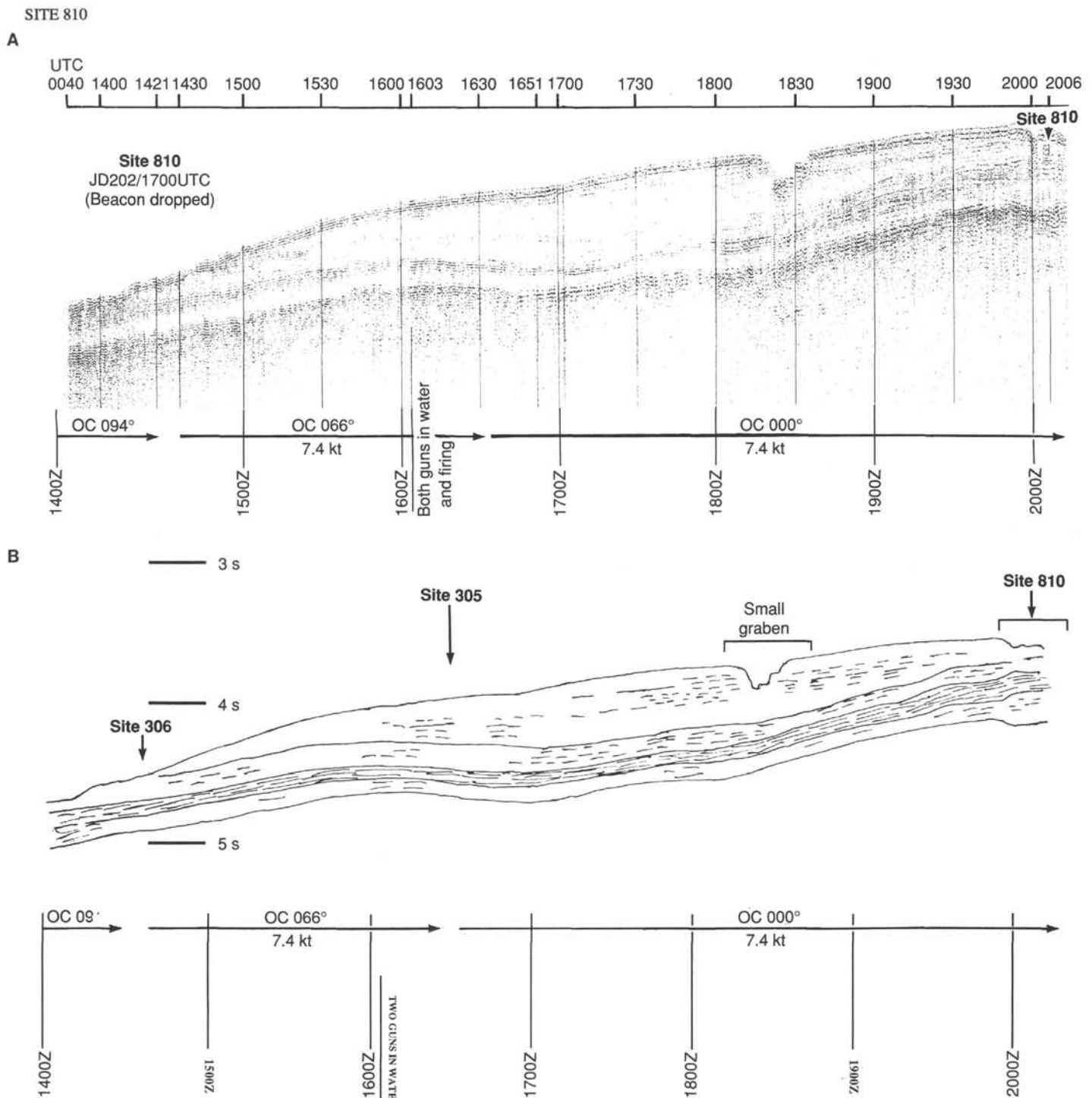


Figure 1. *JOIDES Resolution* profiler record obtained during the approach to Site 810. A. Actual profiler record. B. Tracing of the same record, showing the changing thickness of the sediment cap between Sites 306, 305, and 810. UTC = universal time, coordinated.

Hole 810C

Hole 810C was spudded at 1800 hr on 22 July 1990 using the APC. The intentions were to core with APC and/or XCB, as required, down to the chert reflector in the section. Knowing the exact location of the chert horizon would help to expedite the DCS-cored interval by allowing accurate placement of the DI-BHA bit. Some overlap with APC/XCB cores would also be beneficial in interpreting the effectiveness of the DCS. Also, knowing what the formation properties were like prior to coring with the DCS would help in bit selection and refinement of coring

parameters such as weight-on-bit, bit rotational speed, flow rate, rate of penetration (for controlled feed rate operations), etc.

After spudding, the recovery in Core 132-810C-1H was used to establish an accurate mud line at 2634.1 m. The section was cored from that point down to 2761.2 m or 127.1 mbsf with the APC. The last piston core, 132-810C-15H, did not bleed off indicating incomplete stroke. The barrel was pulled from the sediment using the sand line with no sign of overpull which had been running up to 10,000 lb on previous cores. Upon recovery, the APC shoe was found to be severely damaged on one side. This was firm evidence that the barrel had contacted a chert horizon.

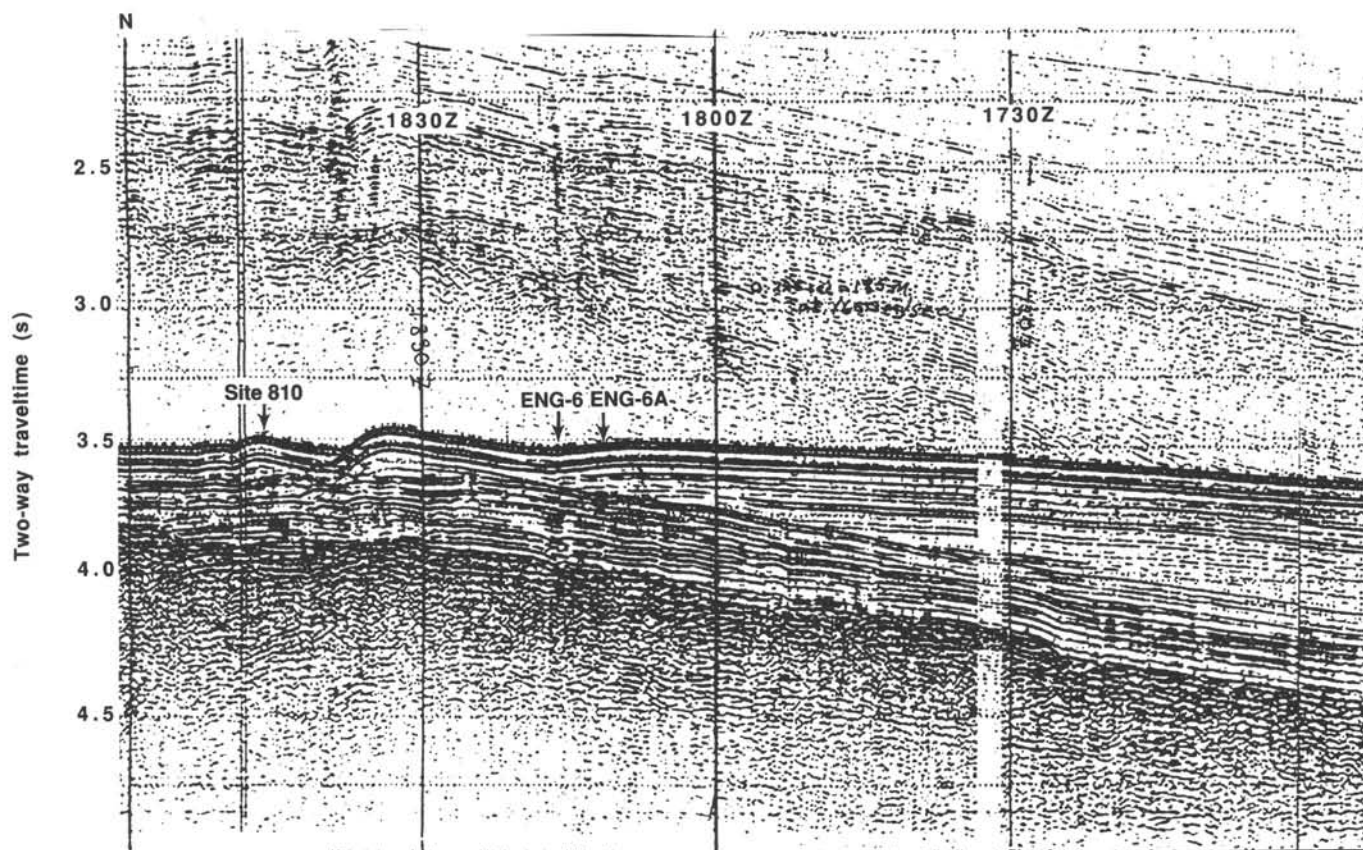


Figure 2. Kana Keoki seismic line 77-03-17, Leg 5. The original target site, ENG-6, is at 1812Z. The equivalent position of Site 810 is actually at about 1840 on this profile.

Although recovery was a respectable 9.88 m, we felt that the barrel most likely did not actually penetrate that far. That belief was later supported by the scientific party which verified that the majority of the core was highly disturbed flow-in material.

Core 132-810C-16X was cut using the XCB system with a polycrystalline diamond compact (PDC) cutting shoe. While washing down the rathole from the previous APC core, a hard surface was encountered after 1.1 m. We assumed that this was indeed the chert layer and that the APC barrel probably had not penetrated beyond that point. Coring on Core 132-810C-16X continued from that point down an additional 9.0 m where we stopped coring. Total depth achieved was 2770.2 m or 136.1 mbsf. Recovery, thanks to a flawlessly performing piston corer-system, was 105.7 percent for the entire calcareous ooze section. The last core cut, using the XCB, recovered 2.92 m of milky white calcareous ooze with some fragmental chert. This core required 40 min of rotating time to cut and at times required up to 18,000 lb weight-on-bit. Hole 810C was officially terminated at 1200 hr on 23 July when the bit arrived on deck.

Hole 810D

The first order of business for Hole 810D was to prepare the modified reentry cone for deployment. Modifications to the cone included the addition of cuttings-diverter pipes and a special cone transition/casing hanger for compatibility with the DI-BHA hardware.

The reentry cone, which had been pre-assembled as much as possible, was moved into position over the moon-pool doors. A total of 48.79 m of 16 in., 75 lb-per-foot, casing was made-up. That would allow 52 m of casing to be emplaced into the seabed,

approximately 10 m less than what was verified as "jet-able" at Hole 810B. The lower end was terminated with a "Texas" weld-on casing shoe. The 16 in. casing hanger was made-up and torqued to 7500 ft-lb. The joint was then tack-welded in four places at 90°. Some difficulty was encountered in landing the casing hanger inside the throat of the reentry cone and the problem was believed to be caused by some welded-on dogs at the base of the hanger. These dogs were meant to engage slots in the cone and provide torsional resistance during the un-jaying operation. After several hours of raising, lowering, and rotating the casing attempting to align the slots we decided that some misalignment of the dogs must be preventing the hanger from landing properly. Since they were judged unnecessary given the weight of the structure and the sticky nature of the sediments the dogs were torch-cut off. After this operation was completed, the hanger was lowered back into the cone and again it would not seat properly. There was continual binding during this process between the casing hanger and the cone transition pipe. The C-ring did not engage so the hanger was picked-up, rotated, and relanded several times in an attempt to get it all the way down on the landing shoulder. After one such landing attempt, a splash was heard. When the hanger was retrieved, the casing was missing. The casing box thread appeared to be machined correctly and there was no visible sign of damage. Grease marks clearly indicated that adequate thread make-up had been achieved. The only answer to the mystery at this time is that the tack welds broke, allowing the casing to rotate and unscrew during the repeated attempts to seat the casing hanger.

While a new casing-string space-out was underway, attention was turned to the other problem of why the hanger was not seating properly. The C-ring was removed to eliminate it as a source of

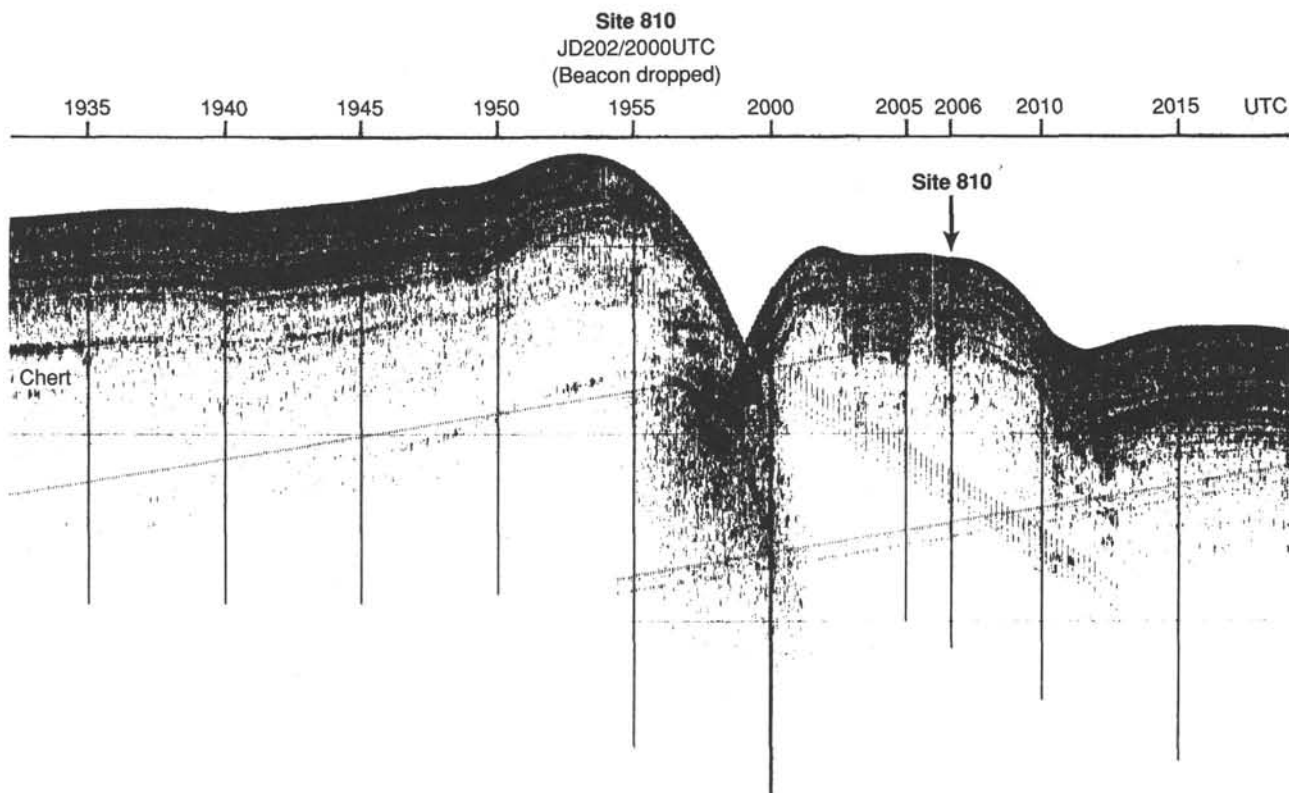


Figure 3. *JOIDES Resolution* 3.5 kHz record obtained in the vicinity of Site 810, showing the “chert reflector” doublet as well as channel-features (hyperbolic echoes) south and north of the site.

the problem. Subsequent to removal of the C-ring, the hanger was lowered into the cone transition and a loud report was heard as the hanger dropped down slightly. The hanger appeared to be correctly shouldered and now in proper position. When picked-up, however, the cone was firmly attached to the hanger, even though no C-ring was installed. Several hours were spent welding the cone and support beams down to the moonpool doors so a good pull could be made to try and unseat the hanger. All efforts proved futile, however, and the exercise was abandoned at 0300 hr on 24 July 1990. We surmised at that time that welds on the outer diameter of the casing hanger body, coupled with welds or eccentricity in the bore of the cone transition-pipe, was responsible for the problem. Since time was critical at this stage, we decided to weld the casing hanger into the cone throat, load up the cone base with as many drums of pig-iron ingots as possible (14 eventually were loaded), and run the cone in the hole without casing. We felt the cone/ingot weight (35,000 lb in water) plus the weight of a 115-m-long DI-BHA (45,000 lb in water) would be enough to achieve tension. Without any skin friction factor applied to the BHA, a factor of safety of 2:1 was achievable.

The modified, ingot-laden, and casing-less reentry cone was deployed and landed on the seafloor at 1300 hr on 24 July 1990, officially spudding Hole 810D. The cone was released from the jay-tool and the drill string was then tripped back to the rig floor.

A DI-BHA was made-up with a 9-7/8 in. DCS-H87F bit, a stabilized bit sub, latched-in center bit, 11-5/8 in. back-off sub assembly, and four stands of 8-1/4 in. drill collars and run in the hole.

In less than 1 hr the vessel was maneuvered over the cone and reentry achieved. The stage was now set for drilling-in and releasing the BHA.

After a straightforward washing operation the BHA apparently landed but no evidence of successful back off was indicated. It appeared that although seated, the two back-off tapers were not contacting each other. Since a C-ring was deployed this time and was not used on the earlier successful back-off sub deployments on Site 809, it was considered a suspect in preventing proper shouldering. Additional weight was applied, up to 25,000 lb, to attempt forcing the C-ring down into the landing seat bore but this only resulted in causing the positive displacement coring motor (PDCM) to stall out. The locking balls, described in Site 809 Operations, were dropped, locking the mud motor. A top-drive torque of up to 20,000 ft-lb was applied, but still no success was achieved at backing-off the nut. We decided at that point to trip the drill string and inspect the downhole hardware. During the trip a spare C-ring was modified with a small bevel to eliminate the square edge which must pass into the landing sleeve bore. This was done to save ship's time when all hardware was recovered on-deck, on the presumption that the C-ring was causing the downhole problem.

At 1630 hr on 25 July 1990 the back-off hardware was recovered on-deck. The C-ring was found properly latched into the groove in the landing seat, as designed. However, the shear pins in the landing seat had sheared out when the BHA was retrieved because the back-off nut had not released. The keys welded into the casing hanger to prevent rotation of the landing seat had also sheared allowing the entire landing seat to spin thus not letting the back-off nut unscrew.

Because the hole was pre-drilled, at this point we elected to break the make-up torque on the back-off nut and run in the hole with an un-torqued assembly. The nut broke out on deck as designed at around 5000–6000 ft-lb of torque and was unscrewed

three-fourth turn to ensure that the threads were not damaged. No problems were anticipated with the "loose" assembly since no rotation would be required to get back to the bottom of the hole.

To allow transmission of torque for unscrewing the back-off nut, the landing sleeve had to be modified. We had the SEDCO welder put beads of hard facing on the outside diameter of the sleeve and on the bottom of the landing shoulder. We felt that this would jam the sleeve into its landing spot tightly enough to allow unscrewing the un-torqued back-off nut. This modified DI-BHA was deployed and reentered into the cone at 0100 hr on 26 July 1990.

After landing the assembly, all attempts at back off were again fruitless. All variations of low and high weight (2,000–40,000 lb), low and high rotational speed (35–100 rpm) were tried, all in vain. Several times the pipe become stuck in the process allowing rotation to take place but not allowing the pipe to be picked up.

Ultimately, after having the pipe stuck for over an hour, the assembly was freed and we decided again to recover the drill string and inspect the hardware. At 1200 hr on 26 July 1990, the back-off assembly was once again at the rig floor. Inspection of the hardware indicated that the C-ring had again latched properly into its groove. The hard facing on the landing seat had done its job and allowed the back-off nut to fully unscrew. The only thing holding the 45,000-lb BHA was fusion or jamming between the two tapers on the landing sleeve and back-off nut. But for this problem, the system had worked as designed. There was no apparent reason for the pipe-sticking problem although later we believed this to be the result of the landing sleeve flaring due to excessive heat and load being applied to the taper. Eventually the outside diameter wore down allowing retrieval from the casing hanger.

Operations at Site 810 were further hampered on this date by a Japanese tuna boat. Buoys supporting fishing lines from this boat were seen off both starboard and port sides aft. The buoys were not drifting free but were obviously fouled on something beneath the ship. We feared that line would get sucked into or fouled on the thruster pods or hydrophones. The captain methodically had these structures raised one at a time. The buoys and attached line ultimately became freed when the BHA was recovered aboard ship.

The third DI-BHA run in the hole had a new landing sleeve, with appropriate hard-facing build-up, and the new beveled C-ring. This was done to conserve rapidly-diminishing operating time and save the time it would take to rebuild the other assembly. The beveled C-ring was not anticipated to be a problem because the BHA was to be drilled down this time to just above the top of the chert reflector, thus supporting the BHA if it should release from the reentry cone. Since some amount of new hole was to be drilled this time the back-off nut was left tightened-up.

The DI-BHA was made up once again, this time with an additional 13.7 m added to space the casing shoe (DI-BHA bit) to within 0.8 m of the chert layer. Reentry was made at 2145 hr on 27 July 1990.

As the back-off assembly landed, a momentary jump in rotary torque to 18,000 ft-lb was witnessed followed by a drop in torque below normal and a subsequent loss of 50,000 lb of BHA weight. The pipe at the rig floor also over-spun as the torque was released. All of these events indicated that the BHA had released this time as designed.

Before tripping the drill string we decided to recover the center bit, thus saving a reentry operation prior to tripping the DCS tubing string. Initial attempts at getting the sinker bar assembly to bottom were to no avail, however, and we feared that the BHA had parted or backed-off about 25 m below the casing shoe.

Eventually the tools were worked to bottom but did not recover the center bit. Upon recovery, the overshot was found to be heavily damaged, providing further evidence of a downhole problem. The drill string was then tripped out of the hole.

On deck, the back-off nut was again discovered to be fused or wedged into the landing sleeve. The nut had indeed backed-off as designed. However, the BHA had fallen out the bottom of the casing hanger when the beveled C-ring failed to shoulder in the landing groove. This particular landing sleeve had been modified during operations at Site 809 to open up the clearance through the inside diameter. This was done when it appeared that the tight, 1/8 in. clearance was causing the DI-BHA assembly to bind up while being drilled-in. As a result, the BHA fell 25 m into the formation when released from the back-off assembly, the assumed multiple chert layers doing little or nothing to impede the fall. Damage to the overshot was obviously the result of setting down on the splined top of the DI-BHA lower back-off assembly.

It was now too late to continue with operations for ultimate DCS deployment, but a back-up site, conventionally cored, could still be drilled. First, additional drill collars were brought up from the riser hold for the contingency site. Then all efforts turned to laying out the DCS tubing string and storing it on top of the riser hold hatch, before the weather, which was threatening, became too rough for handling the joints safely.

Ultimately, because of the approach of Typhoon Steve and the time required both to lay out and stack all of the DCS tubing, and then rig down all heavy DCS hardware (requiring crane operations), the contingency site was canceled and we decided to spend the remaining time attempting to recover the BHA and 12 drill collars left in Hole 810D.

A pilot modification to the 5-1/2 in. FH DI-BHA fishing tool was made and at 1315 hr on 28 July 1990, the entire remaining DI-BHA was successfully recovered from the hole. By 1420 hr on 29 July, all collars had been laid down, and the ship got underway. Since, this was still early for a departure to Guam, even with deteriorating weather, a short box survey of the Shatsky Rise area was conducted.

Shatsky Rise Seismic Survey

Once underway, we steamed south at 4 kt, streamed gear, and turned back over Site 810, increasing speed to 6.5 kt. At this speed, we carried out a seismic survey of the region around a fairly substantial seamount exposing basement at its summit, a few kilometers north of Site 810. We crossed the seamount on a west-to-east course, then turned first south, then southwest, to link back to Site 810. We left Shatsky Rise on a course of 210° steaming at 6.5 kt to obtain a line over the tapering sediment prism on the southwest side of Shatsky Rise, to a depth of 3400 m. We intended to carry this line somewhat further to the southwest, but were deterred by rapidly deteriorating weather conditions, which persuaded the Captain that we should leave the area with all possible speed.

LITHOSTRATIGRAPHY

At Site 810, Holes 810A and 810C, we recovered 129.8 m of Tertiary and Upper Cretaceous nannofossil ooze. Based on foraminifera, the section was complete except for the following hiatuses:

- upper Miocene–lower Eocene
- lower Eocene–upper/lower Paleocene
- lower Paleocene–lower Maestrichtian

The oldest sediment recovered was early Maestrichtian.

The section consisted of nannofossil ooze throughout, and was divided into five units (Fig. 4):

Unit I (0.0–4.2 mbsf; Section 132-810A-1H-1 to -4, 25 cm; Core 132-810C-1H to Section 132-810C-2H-2, 30 cm)

Unit I consists of nannofossil ooze with common to abundant siliceous microfossils: radiolarians, diatoms, and sponge spicules. It is distinguished by its brownish and dark gray colors, and by the apparent cut-and-fill structures (color interfaces at high inclination) suggesting processes of erosion and movement of sediments on the seafloor. This is supported by the fact that Unit I in Hole 810A is at least 75 cm thicker than in Hole 810C, a short distance away. Bioturbation occurs throughout and includes a standard pelagic ichnofossil assemblage (*Planolites*, *Chondrites*).

Unit II (4.2–76.0 mbsf; Section 132-810C-2H, 30 cm, to Section 132-810C-9H-5, 110 cm)

Unit II consists of rather bland nannofossil ooze, with only small contributions from the other common sediment-forming microfossils. It is much lighter colored than Unit I, varying between light gray and white. Distinguishing features include the occurrence of thin, commonly reworked layers of silt to fine sand-sized volcanic ash (Table 2, Fig. 5) and rounded pumice dropstones. These occur as isolated fragments floating in the ooze (Fig. 6), and do not appear to be related to the ash layers. Their roundness suggests reworking prior to deposition. The largest of the ash layers is 14 cm thick and consists of very coarse pumiceous glass, resembling an ash-flow more than an air-fall deposit (Fig. 7). However, the composition of the sample (Table 3), obtained on board ship by X-ray fluorescence analysis, is that of a typical island-arc high-silica rhyodacite. It was probably produced by a large eruption in the Japan-Kuril-Kamchatka area. In the bottom half of Unit II, the light gray to white color alternations take up a distinct rhythmicity. Color transitions between lighter and darker beds occur at 40–80 cm intervals.

The assemblage of planktonic foraminifers throughout this unit becomes increasingly dissolved with increasing depth (see "Biostratigraphy" section, this chapter), and foraminifer abundances decrease substantially with depth in Unit II (Fig. 8). Curiously enough, there is a mixture of well-preserved warm-water and highly corroded cold-water forms. This is unusual because the warmer-water forms tend to be more vulnerable to dissolution than the more robust cold-water forms. We interpret this as mixing of *in-situ* cold-water and warm-water forms, probably transported from the shallower parts of Shatsky Rise. The unit is bioturbated throughout, but contains 2–5 cm thick packages of parallel bands of greenish discoloration, which are invariably associated in smear slide observations with increased amounts of fecal pellets. The green color is probably the result of higher levels of chlorophyll, a highly refractory organic pigment. Similar bands of purplish hue are most likely caused by trace amounts of manganese, perhaps as manganese carbonate (rhodochrosite) stains on carbonate grains. The occurrence of trace organic pigments (chlorophyll) and reduced manganese indicates incomplete homogenization and oxidation of the sediment, possibly as a result of very high sedimentation rates calculated from biostratigraphic data. Trace fossils include *Planolites* and *Chondrites* trace fossils, and a vertical tubular structure which may be *Trichichnus*. *Zoophycos* occurs in Core 132-810C-9H, the bot-

tom-most part of Unit II. Traces of barite and volcanic glass were seen in smear slides throughout Unit II.

Unit III (76.0–99.5 mbsf; Section 132-810C-9H-5, 110 cm, to Section 132-810C-12H-2, 60 cm)

Unit III consists of pale tan to tan clayey nannofossil ooze and calcareous clay. Color alternations form rhythmic bands with a repetition length of 40–80 cm. Clay contents were estimated as high as 70% (calcareous clay) in the darker parts (Fig. 9). The light tan parts are clayey nannofossil ooze (<50% clay). The strongly dissolved appearance of the foraminifers suggests corrosive bottom waters and a lower sedimentation rate. Although shipboard data do not yield high-resolution sedimentation rates, rates appear to decrease downward through Unit III to as little as 2.17 m/m.y. near the base. The unit is strongly bioturbated with a standard assemblage of *Planolites*, *Chondrites*, and *Zoophycos* structures typical of deep sea carbonate oozes, as well as rare *Trichichnus*(?) (Fig. 10) and unexpected *Thalassinoides* structures (Fig. 11). The latter are considered common only in shallower shelf sediments (200–500 m), and not in deep pelagic oozes (Ekdale et al., 1984).

Unit IV (99.5–113.3 mbsf; Section 132-810C-12H-2, 60 cm, to Section 132-810C-13H-5, 40 cm)

Unit IV consists of pale tan nannofossil ooze burrowed throughout by *Planolites*, *Chondrites*, and vertical *Trichichnus*(?) structures. This unit is characterized by very high percentages of large nannofossils. Large nannofossils are typical in lower Eocene–upper Paleocene sediments, but the possibility remains that Unit IV has been winnowed by current activity. Unit IV contains virtually no siliceous microfossils (Fig. 12). Sedimentation rates in Unit IV were low to moderate (2.17–5.5 m/m.y.). Traces of barite occur throughout.

Unit V (113.3–136.1 mbsf; Section 132-810C-13H-5, 40 cm, to Core 132-810C-16X-CC)

Unit V is a white nannofossil ooze with large coccolith plates and 2%–20% foraminifers. Traces of quartz, volcanic glass, barite, and clay occur throughout. Chert nodules occur at 113.5 and 121.25 mbsf in Cores 132-810C-13H and -14H. Large gray-brown chert flakes up to 5 mm thick, 50–75 mm wide, conchoidally fractured, resembling the bottoms of beer bottles, occur in the very top of Core 132-810C-16X (127.1 mbsf). These are probably parts of the chert layer which halted penetration by the piston corer in Core 132-810C-15H. This core consists of 1.25 m of *in situ* sediments and 8 m of soupy cuttings, sucked into the core barrel by the action of the piston during retrieval of this short APC core. In Core 132-810C-16X, we recovered only 2.8 m of pure white ooze, severely disturbed by the rotation of the XCB. Only a few thin biscuits retain the original consistency of the material (firm ooze).

BIOSTRATIGRAPHY

General Remarks

Sediments at Site 810 were retrieved from two holes, 810A and 810C, whereas Hole 810B was washed down. Planktonic foraminifers are generally abundant, but their preservation varies from moderate to poor due to mechanical breakage induced by

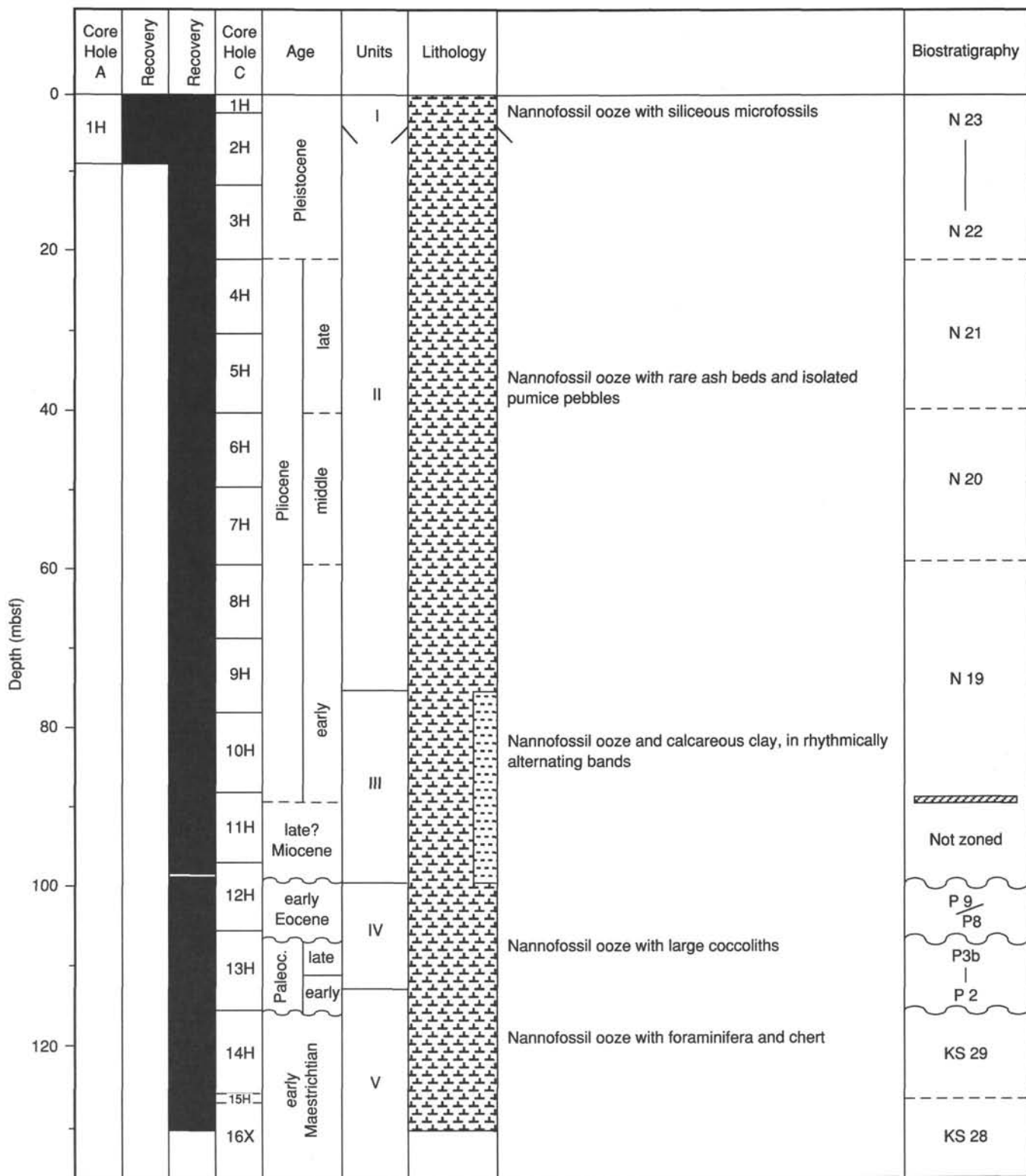


Figure 4. Site summary diagram showing Site 810 core numbers, core recovery, age, lithologic units, graphic lithology, and biostratigraphy vs. sub-bottom depth.

Table 2. Distribution of volcanic ash layers in Hole 810C.

Bed no.	Core, section interval (cm)	Depth (mbsf)	Thickness (cm)	Age	Unit
1	3H-2, 117-118	14.57	1	Pleistocene	II
2	4H-1, 4-6	21.44	2	late Pliocene	II
3	4H-2, 26-27	23.16	1	late Pliocene	II
4	4H-3, 134-135	25.74	1	late Pliocene	II
5	4H-4, 2-83	26.72	1	late Pliocene	II
6	5H-3, 47-48	34.37	1	late Pliocene	II
7	5H-4, 147-149	36.87	2	late Pliocene	II
8	5H-5, 64-65	37.54	1	late Pliocene	II
9	6H-1, 12-20	40.52	8	middle Pliocene	II
10	6H-1, 43-44	40.83	1	middle Pliocene	II
^a 11	6H-6, 18-32	48.08	14	middle Pliocene	II
12	8H-2, 90-91	62.30	1	early Pliocene	II
13	9H-1, 54-55	69.44	1	early Pliocene	II

^a Analysis given in Table 3.

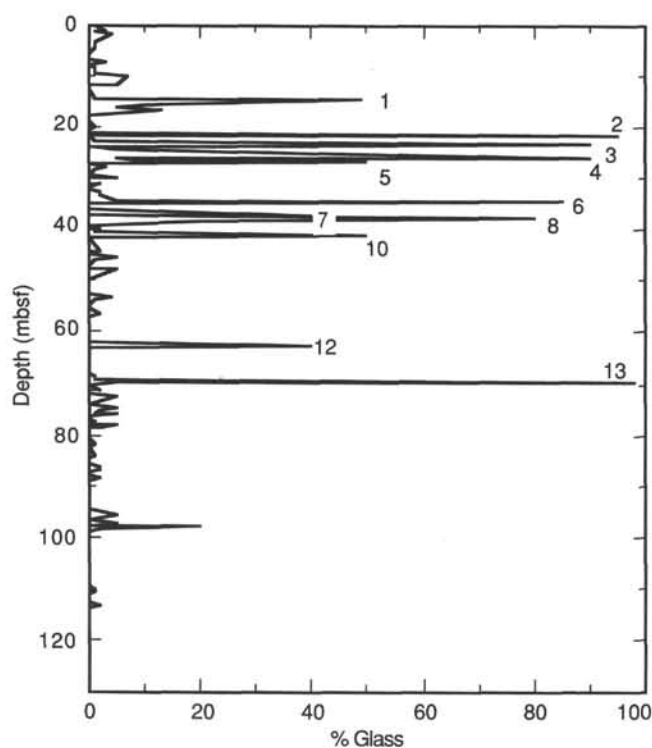


Figure 5. Abundance of volcanic glass in Hole 810C, estimated from smear slide observations. Ash layers listed in Table 2 are individually labelled. No smear slides of ash layers 9 and 11 were made.

either transport or dissolution. The last feature, identified by empty shells or by thinned walls in several, thick-shelled species, deviates from normal dissolution patterns as the site, located at 2634.1 m water depth, was well above the carbonate compensation depth (CCD). This poses a question in interpreting why dissolution occurred at such shallow depth. The problem of transport and dissolution combined renders the age attributions as tentative.

Hole 810A

One core was retrieved at this hole with 100% recovery. Planktonic foraminifers are abundant but partially dissolved. Sample 132-810A-1H-CC yielded a fauna dominated by *Globorotalia inflata*. Common species are *Truncorotalia truncorotaloi-*

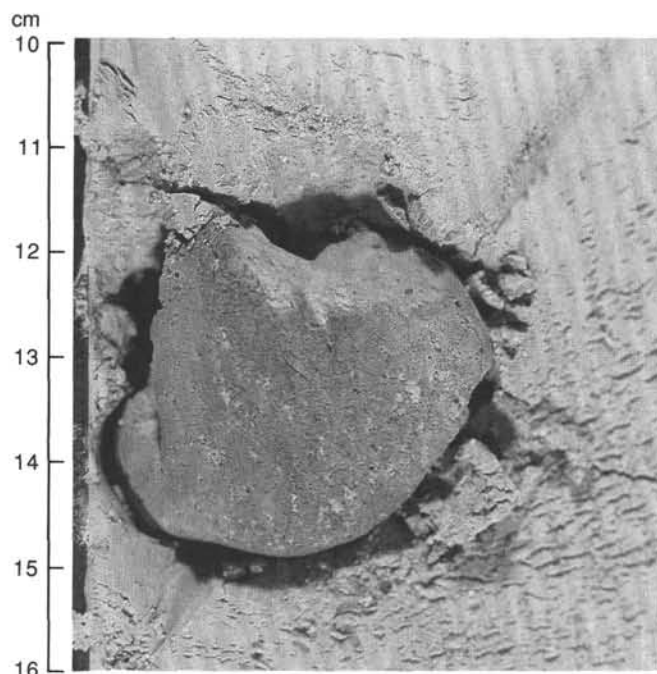


Figure 6. Close-up photograph of isolated pumice dropstone in Core 132-810C-2H-6, 13 cm.

des pachythea, *Globorotalia crassaformis ronda*, and *G. crassaformis oceanica*. A few *Truncorotalia tosaensis* are also recorded associated with *Globorotalia hirsuta*, *G. tumida*, *G. unguata*, *Pulleniatina obliqueloculata*, *Globigerinoides ruber*, and *G. gomitulus*. *Neogloboquadrina pachyderma* is present but rare.

This assemblage seems to indicate an early Pleistocene age, however, it exhibits a mixed warm- and cold-temperate character. The mixed nature of the planktonic fauna is also reflected in the different preservation of benthic foraminifers suggesting some transport from shallower depths.

Hole 810C

Over 100 m of sediments were recovered in Hole 810C with 100% recovery rate. The uppermost 21.4 mbsf yield abundant and diversified planktonic assemblages, which, however, are alternatively dominated by different taxa: *Truncorotalia truncatulinoides* associated with common warm-water indicators (*G. tumida*, *G. menardii*, *Globigerinella aequilateralis*, *Globigerinoides sacculifer*, among others) occur in Sample 132-810C-1H-CC; *Globorotalia inflata* dominates the assemblage in Sample 132-810C-2H-CC, which also contains some warm-water indicators but very rare *T. truncatulinoides*; *Pulleniatina* spp., the *Globorotalia tumida* group, and *Globorotalia crassaformis* are the most frequent taxa in Sample 132-810C-3H-CC. These faunal differences indicate a mixture of assemblages from apparently different horizons of Pleistocene age which were deposited under different environmental regimes (warmer to cooler). This is corroborated by the benthic foraminifer assemblage which contains an autochthonous fauna that is characteristic of lower bathyal water depths in addition to elements from habitats much shallower than present water depth. The poor preservation and strong fragmentation of both planktonic and benthic foraminifers is consistent with the transport hypothesis.

The occurrence of *Truncorotalia tosaensis tenuitheca* and *T. pachythea* in Sample 132-810C-3H-CC together with the ab-

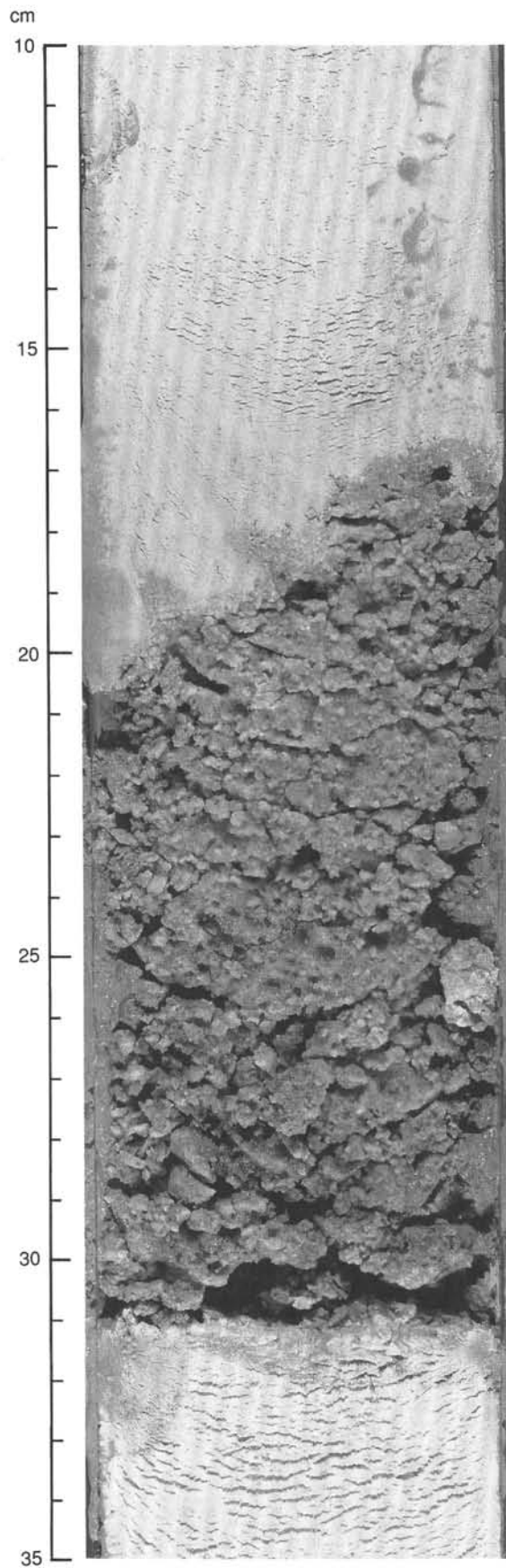


Figure 7. Close-up photograph of coarse pumiceous ash bed in Core 132-810C-6H-6.

Table 3. Shipboard XRF analysis of volcanic ash Sample 810C-6H-6, 19–21 cm.

TiO ₂	0.38	
Al ₂ O ₃	15.33	
Fe ₂ O ₃	0.38	
^a FeO	2.09	
MnO	0.10	
MgO	0.65	
CaO	3.48	
Na ₂ O	4.75	
K ₂ O	1.41	
P ₂ O ₅	0.07	
	101.49	
LOI	-2.10	
^a Mg#	0.357	
CIPW	Norm ^a	
Q	30.25	
C	0.00	
Or	8.32	
Ab	40.16	
An	16.33	
Wo	0.19	
En	Di	0.07
Fs		0.12
En	Hy	1.68
Fs		
Fs		2.78
Mt		0.55
Il		0.72
Ap		0.16

^a Computed assuming $Fe^{2+}/(Fe^{2+} + Fe^{3+}) = 0.86$.

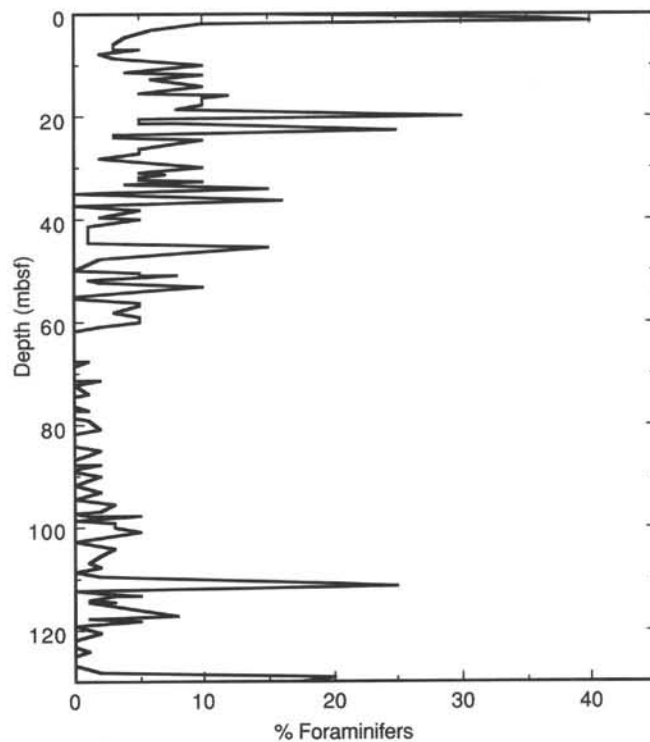


Figure 8. Abundance of foraminifers in Hole 810C, estimated from smear slides.

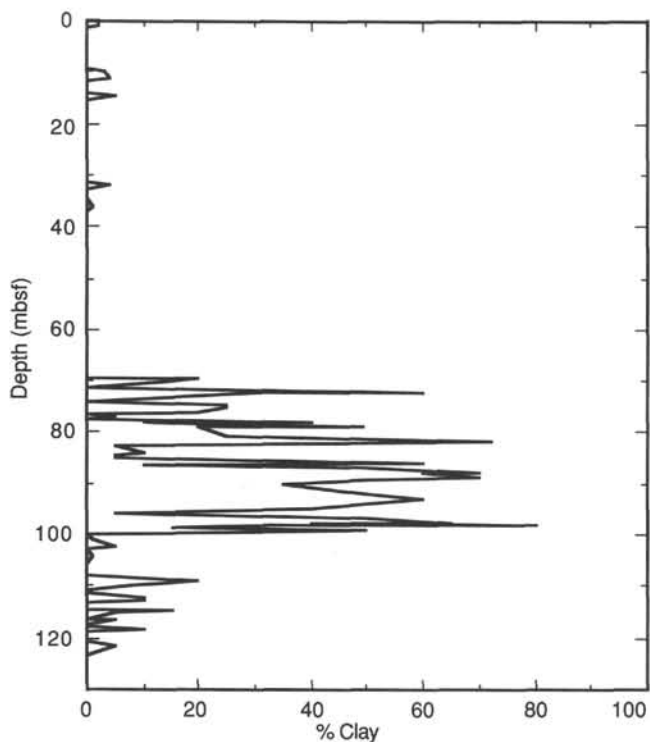


Figure 9. Abundance of clay in Hole 810C, estimated from smear slides.



Figure 10. Close-up photograph of pyritized worm burrow in Core 132-810C-3H-1, 80–83 cm.

sence of typical *T. truncatulinoidea* indicates that the age of the bottom of Core 132-810C-3H is close to the Pleistocene/Pliocene boundary. The presence of *Discoaster broueri*, the last occurrence of which marks the end of the Pliocene, in Sample 132-810C-3H-4, 120 cm, corroborates the Pliocene age at the bottom of Core 132-810C-3H, although reworking cannot be ruled out.

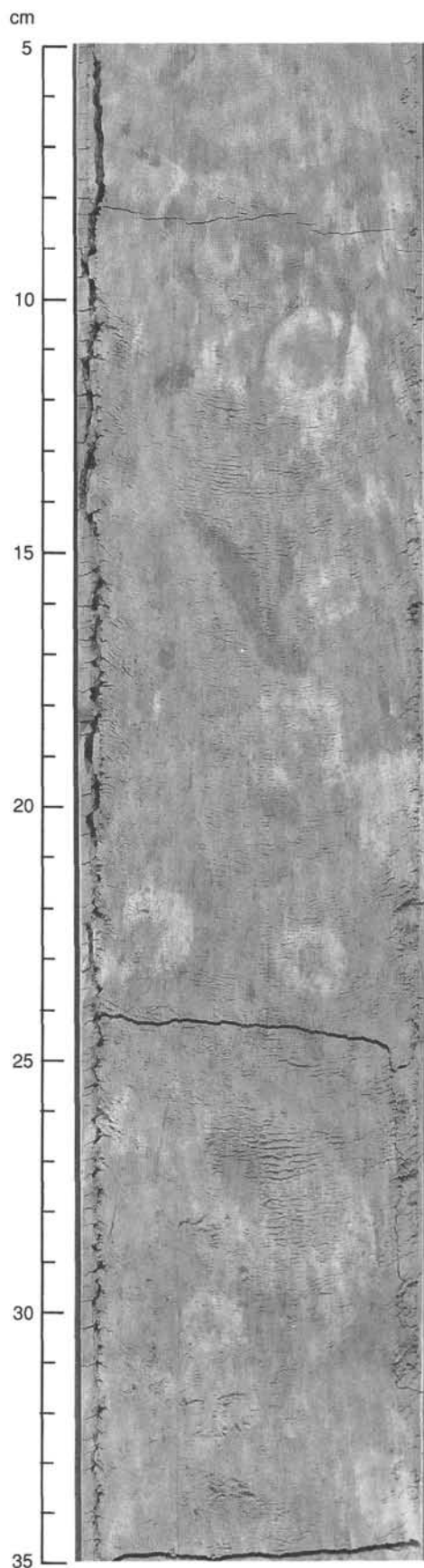


Figure 11. Close-up photograph of Interval 132-810C-10H-6, 5–35 cm, showing extensive bioturbation with *Thalassinoides* trace fossils.

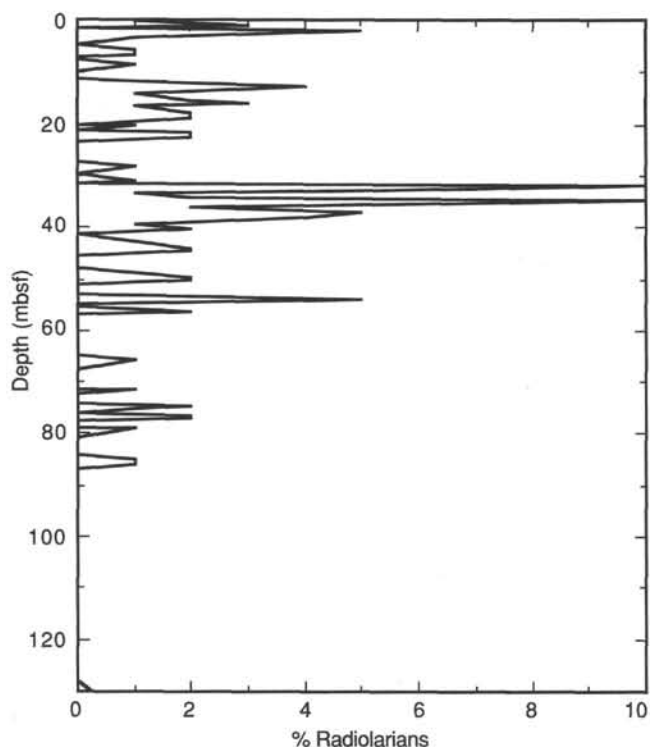


Figure 12. Abundance of radiolarians in Hole 810C, estimated from smear slides.

A few radiolarians are recorded in the uppermost two cores and rare diatoms in Core 132-810C-1H. Volcanic glass associated with pumice occurs in abundance in Core 132-810C-2H, whereas glass is much rarer in the uppermost core.

The interval from Core 132-810C-4H to -10H-CC seems to span the entire Pliocene. Preservation of planktonic foraminifers becomes progressively worse downhole with maximum dissolution in Cores 132-810C-9H and -10H. Increasing dissolution is associated with a decreased abundance of planktonic foraminifers of the pertinent age, whereas reworked forms increase in numbers and in age. These conditions combined are maximal in Core 132-810C-10H, where planktonic foraminifers of middle Miocene, Oligocene, early Eocene, and late Paleocene occur together with a small, mainly dissolved assemblage of early Pliocene age.

Assemblages from Cores 132-810C-4H and -5H are tentatively attributed to Zone N21 (late Pliocene); from Cores 132-810C-6H to -7H to Zone N20 (middle? Pliocene) based on the presence of *Globorotalia puncticulata* and *G. crassaformis* in the absence of *Globorotalia inflata*; from Cores 132-810C-8H to -10H to Zone N19 (early Pliocene) based on the co-occurrence of *Globorotalia margaritae* and *Globigerina nepenthes*.

Benthic foraminifers are very similar in species composition to the Pleistocene assemblages. Common species include *Cibicides wuellerstorfi*, *Uvigerina peregrina*, *Oridorsalis umbonatus*, and *Sphaeroidina bulloides*, among others, but they are always associated with shallow-water forms such as large nodosariids, *Glandulina*, and even *Quinqueloculina*, and thus indicate redeposition from shallower environments.

Radiolarians are common only in Core 132-810C-5H, whereas in the other cores, if present, they are rare. Diatoms are very rare, but crystals of clinoptilolite are common to extremely abundant beginning in Core 132-810C-7H downward. Rare ornamented ostracods and few to common fish remains occur throughout. Volcanic glass is recorded in Cores 132-810C-7H through -9H but is never abundant.

Planktonic foraminifer assemblages from Core 132-810C-11H-CC are Miocene in age, possibly late Miocene, based on the co-occurrence of *Globigerina nepenthes* and *Globoquadrina dehiscens*. A more precise age could not be determined because of the absence of other age-diagnostic species. This assemblage is the most dissolved of the entire hole. In continuity with the trend described for the Pliocene, the foraminifer assemblage of Miocene age in Core 132-810C-11H is depauperate because of dissolution, whereas reworked species, here belonging to the early Eocene and Late Cretaceous, increase in abundance.

Benthic foraminifers are common but strongly fragmented and are associated with common echinoid spines. Radiolarians and diatoms are absent, but clinoptilolite crystals are particularly abundant. Moreover, the washed residue of Sample 132-810C-11H-CC contains possible "histricospherids" with calcareous shells in abundance. Other minerals and pyrite are also common.

A major unconformity occurs within Core 132-810C-12H in Section 2 where possibly late Miocene sediments rest on early Eocene layers without any noticeable lithologic change. The planktonic foraminifer assemblage from Sample 132-810C-12H-CC belongs to the top of Zone P8 or to the base of Zone P9, both of late early Eocene age, based on the co-occurrence of *Morozovella aragonensis* (very abundant), *Morozovella caucasica*, *Acarinina pentacamerata*, "*Globigerinatheka*" *senni*, *Subbotina higginsii*, and *Turborotalia frontosa*. Reworking from early Eocene Zone P6 and possibly the late Paleocene is testified to by the presence of a few *Morozovella edgari*, *Acarinina mckannai*, *Acarinina subsphaerica*, and *Morozovella simulatilis*, among others, but it is a minor feature in comparison with reworking in the upper part of the sequence. Preservation of planktonic foraminifers is moderate to good with some forms of chalky aspect and others recrystallized. Benthic foraminifers and other organisms are rare or absent.

Core 132-810C-13H contains two unconformities, one between Sections 1 and 2, where late early Eocene Zone P8 strata rest on early late Paleocene Zone P3b sediments, and a second at 45 cm in Section 132-810C-13H-5 where sediments attributed to early late Paleocene Zones P2/P3a rest on early Maestrichtian strata. Minor changes in color mark the unconformities, especially the lower one that changes from light pink in the Paleocene to white in the Cretaceous.

The planktonic foraminiferal assemblages of the Paleocene interval are attributed to Zone P3b (*Morozovella pusilla* Zone) from Section 132-810C-13H-2 to Sample 132-810C-13H-4, 137 cm, and to Zone P3a (*Morozovella angulata* Zone) from Sample 132-810C-13H-4, 137 cm, to Sample 132-810C-13H-5, 18 cm, whereas the lowest 25 cm above the contact with the Cretaceous possibly belong to either Zone P2 (*Morozovella uncinata* Zone) or straddle the P2/P3a zonal boundary of late early to early late Paleocene age. Zonal attributions are based on the occurrence of zonal markers. This apparently normal succession of faunas and bioevents is disrupted by a series of interbedded slumped layers and by the strong mixing of older Paleocene ages and the Late Cretaceous. Apparent size sorting is occasionally observed. Beside these depositional disturbances, planktonic foraminifer faunas from this interval are well diversified, abundant, and fairly well preserved.

Benthic foraminifers are rare but include lower-bathyal dwellers such as *Aragonia trinitatis*, *Nuttallites*, and thin, elongated stilostomellids, in addition to a few forms from shallower habitats. Fish remains are rare and siliceous organisms are absent.

The white chalk recovered from Cores 132-810C-13H-5, 45 cm, through 132-810C-15H yielded rich, well-diversified assemblages of early Maestrichtian *Globotruncana aegyptiaca* Zone (Zone KS29) and of early Maestrichtian *Globotruncanella hava-*

nensis Zone (Zone KS28) in Core 132-810C-16X. Preservation of planktonic foraminifers is moderate to fair throughout. Re-working is absent, but strong downhole contamination was observed in the core catcher samples of Cores 132-810C-15H and -16X due to drilling disturbance after hitting the first chert nodules and/or layers somewhere within in Core 132-810C-15H at 127.1 mbsf.

Benthic foraminifers are rare to few, indicative of lower bathyal environment, and have holes in their shells due to predators. Rare to few fish remains occur throughout.

Biostratigraphy and age attributions of the sedimentary sequence recovered in Hole 810C are reported in Figure 13.

A peculiarity of the dissolution facies in Hole 810C is the fact that the forms which underwent major dissolution are those considered less susceptible to solution, whereas the warm, near-surface dwellers such as *Orbulina*, *Globigerinoides*, etc., exhibit less pronounced or no solution effects. This speaks in favor of mixing from shallower depths, but also suggests that during warmer climatic conditions, the foraminiferal lysocline possibly deepened in the Shatsky Rise area.

The stratigraphic succession encountered in Hole 810C is similar in several ways to that described from the nearby Sites 305 and 310. In fact, two major hiatuses bound the early Eocene strata, and another hiatus separates the latest early Paleocene from late Maestrichtian strata. The differences concern mainly the extent of hiatuses and/or the age of the sediments recovered. In fact, faunal fragmentation due to dissolution was described from both Sites 305 and 310 in the Pleistocene and the entire interval from Pleistocene to late Miocene is identical at all three sites (Vincent, 1975); moreover, mixed Paleocene assemblages of Zones P3b to P2 are recorded by Luterbacher (1975) at Site 305. On the contrary, middle Miocene, Oligocene to middle Eocene, and late Maestrichtian faunas present at Sites 305 and 310 (Larson, Moberly, et al., 1975) are absent in Hole 810C.

PALEOMAGNETISM

Introduction

The paleomagnetic measurements which were made with the cryogenic magnetometer on the working-half of split-cores show distinct normal and reversed polarity patterns. The magnetic polarity reversals are identified as normal polarity for negative values of inclination and reversed polarity for positive values of inclination (Fig. 14). The sequence of magnetic polarity reversals observed at Site 810 extend from the Brunhes to the Maestrichtian, according to foraminiferal biostratigraphy. There are several major and minor hiatuses evident in the interpreted magnetic record. Correlations between magnetic reversal patterns based on inclination values and foraminiferal biostratigraphy allow the identification of magnetic chrons in the uppermost sedimentary sequence, although identifications in the deeper section was more difficult. Patterns in inclination recorded in the sediment have been compared with physical property and lithostratigraphic information to identify zones of disturbance or re-working which would disrupt the magnetic anomaly pattern. Magnetic susceptibility data collected at Site 810 are discussed in the "Physical Properties" section (this chapter).

The normal remanent magnetism of the sediment cores was analyzed along with data from progressive alternating field demagnetization steps of 5 and 10 mT run on each core section. Summary plots of inclination are provided to illustrate the sequence of magnetic polarity reversals at Site 810.

The first core recovered contains a much abbreviated or missing Brunhes chron. The Jaramillo event is most likely missing but

may be observed as a poorly expressed change in inclination near 0.4–0.8 mbsf or 1.2–1.4 mbsf. These shifts in inclination are each marked by changes in the texture of the sediments, as observed in the core photos, and by sharp peaks in magnetic susceptibility, compressional wave velocity, and GRAPE bulk density within this zone. A long period of negative inclination throughout Core 132-810C-2H and the upper part of Core 132-810C-3H is interpreted as the reversed polarity interval corresponding to the upper Matuyama (Fig. 15). A shift to normal polarity at 18.2 mbsf, is interpreted as the Olduvai event and the boundary between the Pleistocene and late Pliocene. The biostratigraphic summary places this boundary at the bottom of Core 132-810C-3H at 21.5 mbsf in close agreement with the magnetic interpretation. Normal polarity is observed from Section 132-810C-3H-05 to the top of Section 132-810C-3H-7 where a short return to reversed polarity occurs. The inclinations in Cores 132-810C-4H and 132-810C-5H are dominantly positive.

The polarity is reversed for most of Core 132-810C-6H to the top of Section 132-810C-6H-5 (Fig. 16). The termination of this interval downhole is disrupted near 47.5 mbsf, and again above a 14 cm ash bed, located in Section 132-810C-6H-6. A messy magnetic transition across this zone is followed by a short normal polarity interval extending from the bottom of Core 132-810C-6H to the top of Core 132-810C-7H. This normal interval extends to 51.0 mbsf where a transition to reversed polarity occurs near a thin dark layer in Section 132-810C-7H-01, 110 cm. The data collected from the more deeply buried intervals at Site 810 are illustrated in Figures 16–18.

PHYSICAL PROPERTIES

Introduction

The purpose of using the APC to recover the upper sedimentary section at Site 810 was to confirm that the skin friction between the sediment and seafloor assembly would be sufficient to allow tensioning of the DCS. A program of shear strength testing was carried out using a hand-held Torvane device inserted into the cut-end of each core-section perpendicular to bedding. This testing procedure provided information quickly without significantly slowing the flow of material through the core lab or disrupting the rest of the scientific/engineering routine.

Following shear testing, the core sections were passed through the multi-sensor track (MST) using a protocol designed to obtain anticipated proxy climatic signals from the high-resolution magnetic susceptibility, *p*-wave logger (PWL), and GRAPE bulk density data. The magnetic-susceptibility data were collected for 10 s at a measurement interval of 3 cm. The magnetic-susceptibility sampling density resulted in multiple GRAPE bulk-density determinations.

Whole-round samples for consolidation testing were taken after the cores passed through the MST. Whole-round samples were not taken for interstitial water and organic geochemistry determinations at Site 810.

The physical properties program at Site 810 was designed as a pilot study for a more intensive high-resolution sampling effort to be conducted post-cruise. Measurements of compressional wave velocity using the Hamilton Frame were omitted because of a shortage of personnel on Leg 132. However, compressional wave velocity data were obtained using the PWL. Emphasis was placed on measurements of index properties at approximately 50 cm spacing to compare discrete values with continuous GRAPE bulk-density, PWL, and magnetic susceptibility measurements. Other objectives were to assist in determining mass accumulation

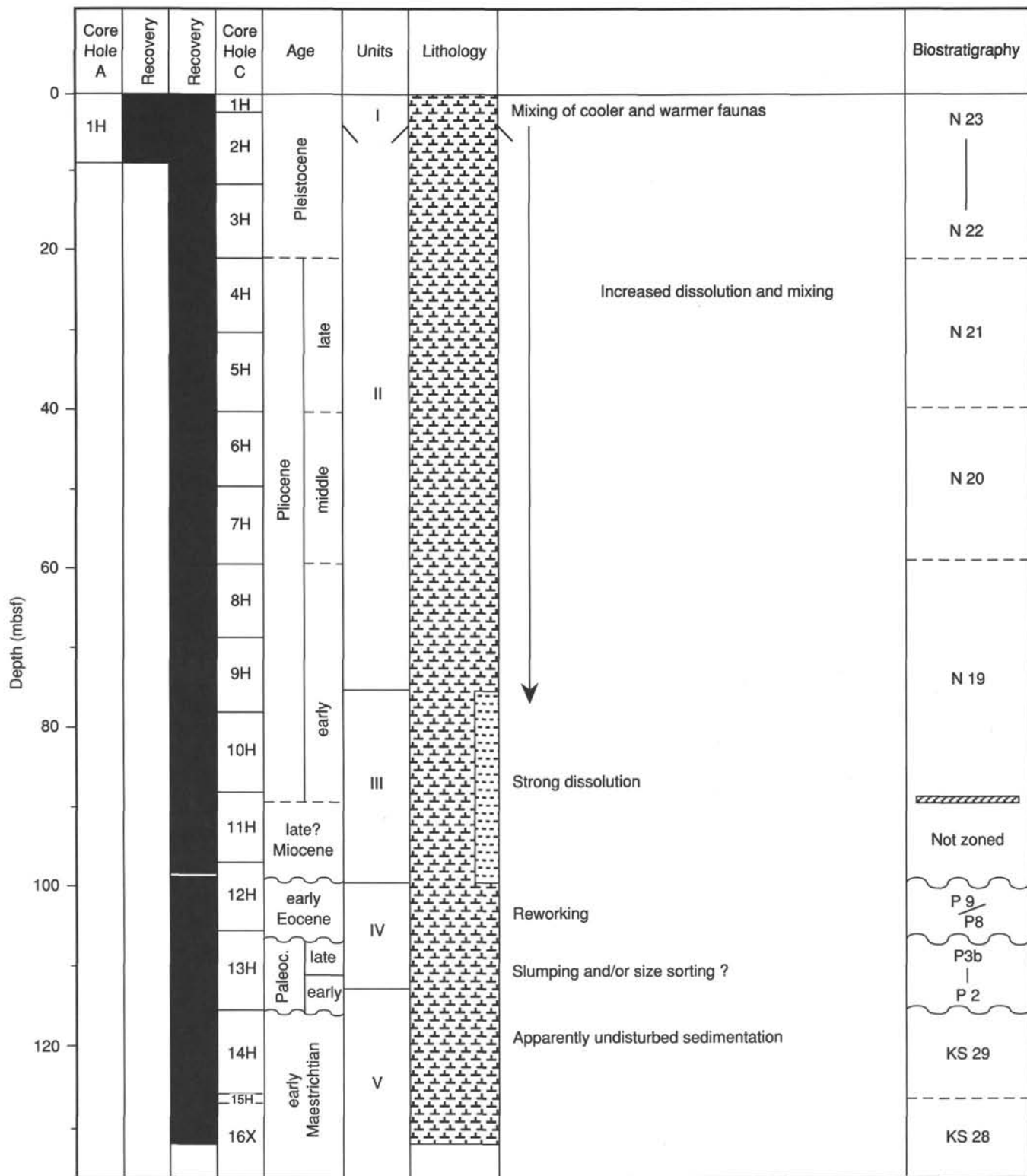


Figure 13. Biostratigraphy and age attributions of the sedimentary sequence recovered in Hole 810C.

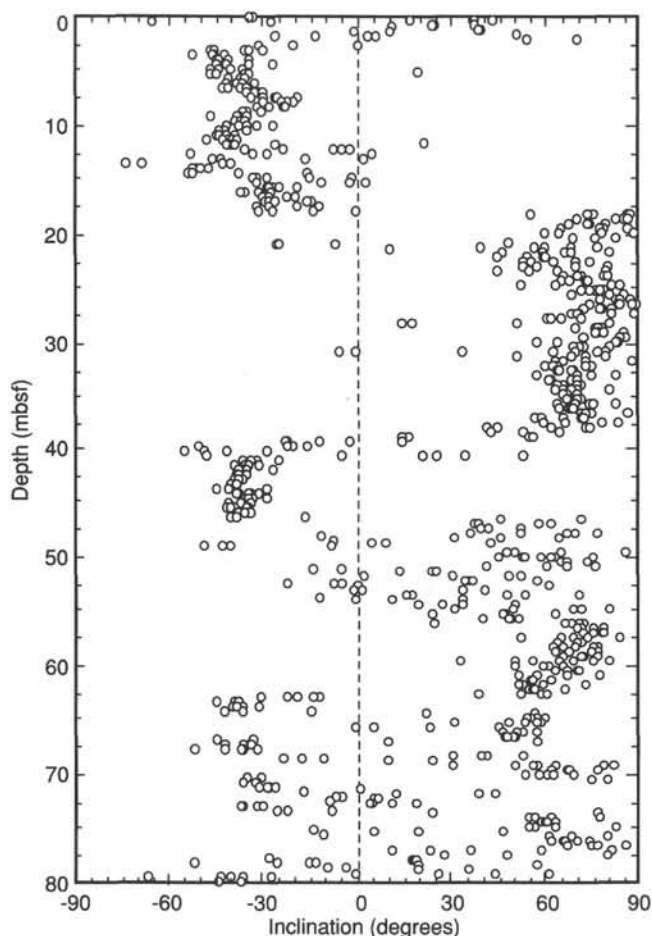


Figure 14. Inclination data for natural remanent magnetism of cores between the mud line and 80 mbsf at Site 810.

rates, correlate with changes in carbonate content, and aid in the identification of hiatuses through the post-cruise determination of a geotechnical stratigraphy for this site.

Vane Shear Strength

The shear strength of carbonate sediments in the upper few meters of sediment is typically in the range of 25–30 kPa (Kenter and Schlager, 1989; Lee, 1982), although it can be highly variable downhole because of diagenetic effects, variations in carbonate content, and the influence of effective overburden stress. Strength in carbonate sediments results from the mechanical interaction of individual carbonate grains during shearing (Lee, 1982). Vane shear testing of marine sediment was discussed by Bryant et al. (1981). They compiled early DSDP results to show that the shear strengths measured on nannofossil ooze in the split cores (parallel to bedding) were often 2–3 times higher than those obtained when the vane was inserted into the end of the core-liner before splitting. They observed that the strengths measured in sediment from the upper 10 m of the seafloor ranged between 2 and 100 kPa, and were greater than 100–240 kPa between 100 and 250 mbsf. However, the impact of drilling conditions and sediment diagenesis set important constraints on their data.

Torvane shear strength data, collected perpendicular to bedding at the ends of whole-round core sections are listed in Table 4 and illustrated in Figure 19. Figure 19A presents strength data in kilopascals, whereas Figure 19B uses units of tons/square foot for the benefit of conversion to kip/square foot (divide by 2) for engineering calculations. Vane shear strength data collected with

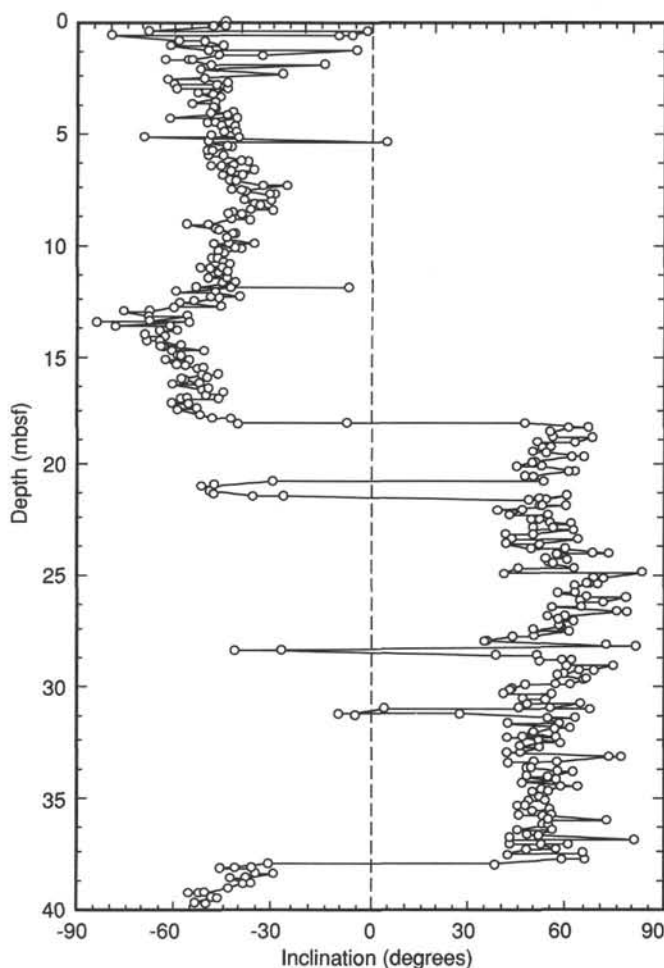


Figure 15. Plot of magnetic inclination data for the interval between the seafloor and 40 mbsf at Hole 810C. Inclination data after AF demagnetization of 10 mT.

the Wykeham-Farrance motorized vane device parallel to bedding on the working half of the split core are listed in Table 5 and illustrated in Figure 20. The maximum shear strength at Site 810 was 121 kPa at 21.0 mbsf, measured in the split-core.

The Torvane shear strength increases gradually to about 70 kPa at 75 mbsf before gradually decreasing to values similar to the upper part of the section at about 110 mbsf. The maximum value corresponds closely to the lower boundary of Lithostratigraphic Unit II, although average strengths of 50 kPa continue to occur throughout Unit III, a clayey nannofossil ooze and calcareous clay. Shear strength decreases markedly below 100 mbsf in the nannofossil ooze of Lithostratigraphic Units IV and V. The apparent underconsolidation of these units may result from disturbance during coring which breaks down the natural fabric of the granular calcareous skeletons. Evidence of slumping and extensive bioturbation in these units may also have contributed to the low shear strengths observed.

The shear strengths measured from the split core are less regular than the Torvane strengths but exhibit a similar decrease in strength below 100 mbsf. Some of the variability in the data results from changes in water content, dissolution of microfossils, or increases in clay content over the intervals sampled.

Index Properties

Gravimetric determinations of index properties were made at approximately 50 cm intervals. This spacing was sufficient to

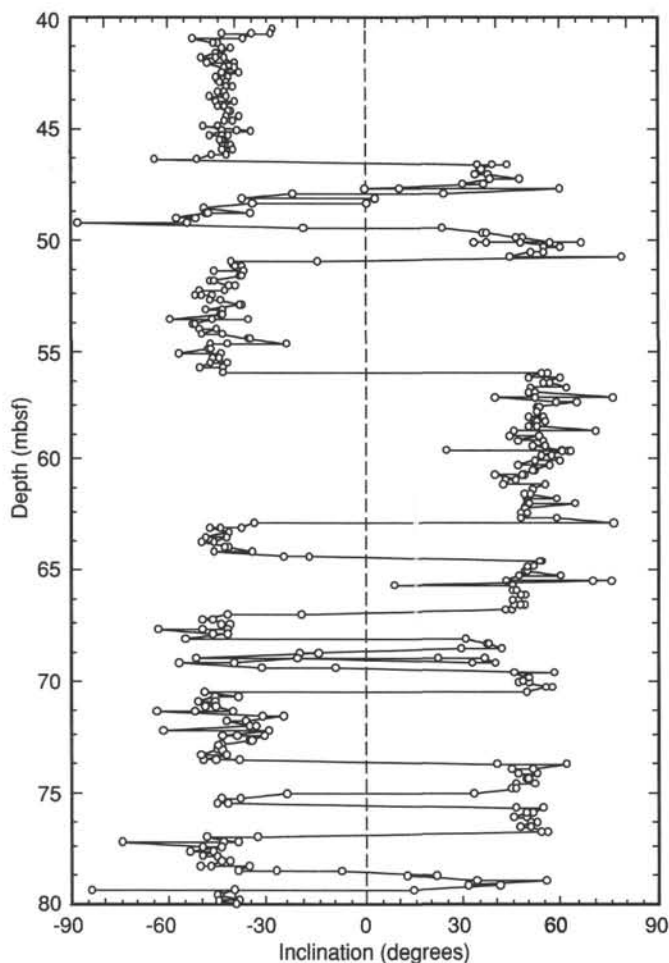


Figure 16. Plot of magnetic inclination data for the interval between 40 and 80 mbsf at Hole 810C. Inclination data after AF demagnetization of 10 mT.

quantify subtle changes in physical properties due to mineralogical and diagenetic variability within individual lithostratigraphic units. Trends in discrete measurements are used to locate possible hiatuses and divide the sedimentary column into subunits exhibiting similar gradients in physical properties. The wet- and dry-bulk density and grain density data collected at Site 810 are listed in Table 6 and illustrated in Figure 21. The data on porosity and water content are in Table 7 and in Figure 22. The overall trends observed at Site 810 to 99.5 mbsf are gradually increasing wet- and dry-bulk density and decreasing porosity and water content with increasing overburden pressure (burial). An abrupt down-hole change in physical properties occurs in Core 132-12H. Section 132-12H-2 is marked by an increase in wet- and dry-bulk densities from 1.70 to 1.86 g/cm³ and 1.03 to 1.30 g/cm³, respectively. A 10% decrease in porosity from 65% to 55% and a decrease in water content from 66.0% to 43.7% (%dry-sample weight) or 38.9% to 30.4% (%wet-sample weight) are also observed. These changes are indicative of a substantial erosional hiatus which is dated biostratigraphically as separating the upper Miocene(?) from upper lower Eocene sediments. This change is also identified as the boundary between Lithostratigraphic Units III and IV. Another abrupt change is observed in Core 132-810C-13H at about 106 mbsf when the gradients of index properties reverse. The sediments exhibit deformation structures and color variation throughout Sections 132-810C-13H-1 to 13H-4. Several rapid inflections in index-property trends are also observed in

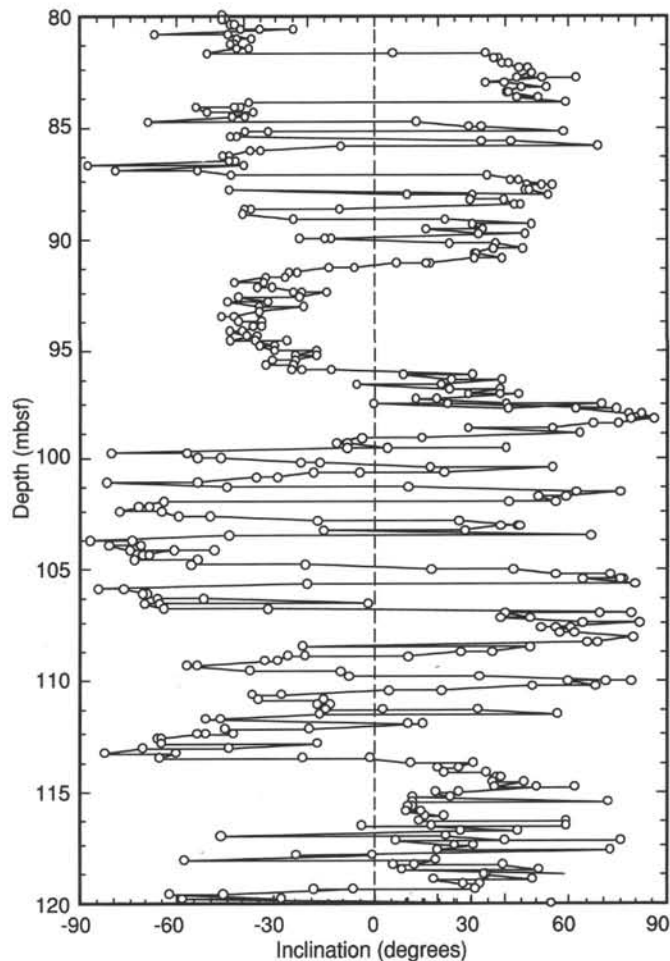


Figure 17. Plot of magnetic inclination data for the interval between 80 and 120 mbsf at Hole 810C. Inclination data after AF demagnetization of 10 mT.

Section 132-810C-13H-5 near the biostratigraphic boundary between the late Paleocene and lower Maestrichtian and the transition to Lithostratigraphic Unit V at 113.3 mbsf. Chert was encountered at 120 and 127.1 mbsf, where APC recovery ceased.

Magnetic Susceptibility

The MST was used extensively at Site 810 to obtain high-resolution profiles of magnetic susceptibility, GRAPE bulk density, and compressional-wave velocity, using the PWL. The physical-properties scientist on Leg 132 also functioned as the paleomagnetist, so these data were integrated with the lithologic descriptions to determine the possible hiatuses in the sedimentary record at Site 810.

The importance of the eolian flux to marine sequences in the North Pacific has been discussed by several researchers (see Rea and Janecek, 1981; Janecek and Rea, 1984; Pias and Leinen, 1984; and Rea and Leinen, 1988; among others). Eolian material represents a significant source of sediment over an extensive geographic region through the Neogene and should be reflected in the variability of the physical properties record collected at Site 810.

Magnetic susceptibility data were collected at 3 cm intervals in the hope of acquiring a unique record to correlate fluxes of eolian material (clay minerals) with susceptibility peaks. Magnetic susceptibility data have been proposed as a proxy measure of climate (Hovan et al., 1989) and may provide a direct link

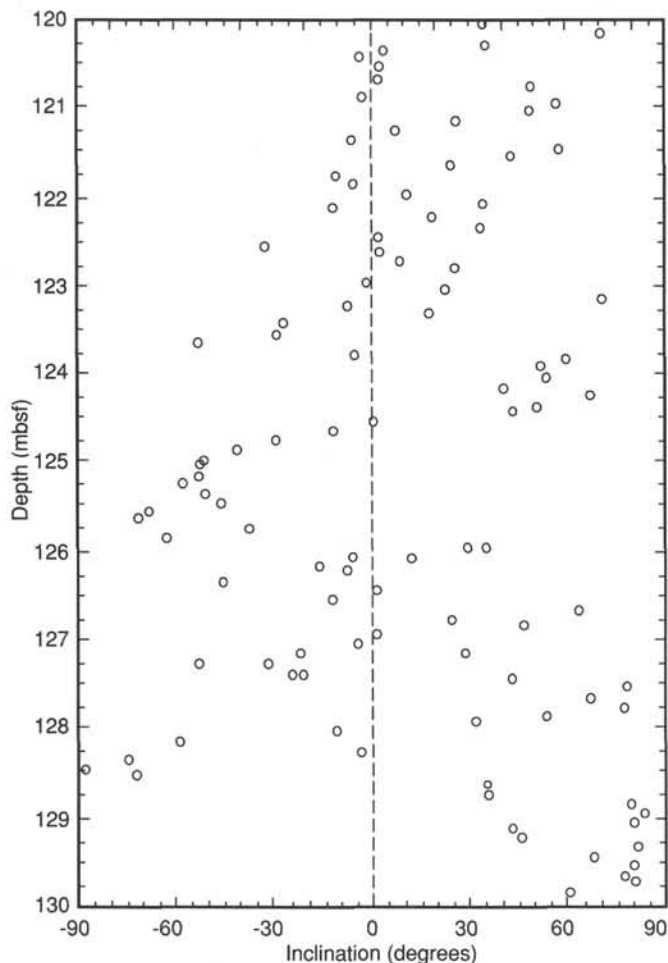


Figure 18. Plot of magnetic inclination data for the interval between 120 mbsf and the base of Hole 810C. Inclination data after AF demagnetization of 10 mT.

between the marine record and the terrestrial record of the loess sequences at Xifeng and Luochuan in central China, where the earliest loess appears near the Gauss/Matuyama boundary (Kukla et al., 1988; Hovan et al., 1989). Kukla et al. (1988) determined that the magnetic susceptibility of loess and interbedded soils varies with the degree of pedogenesis and closely parallels the oxygen-isotope fluctuations in deep-sea sediments (Kukla et al., 1988; Hovan et al., 1989).

The volume magnetic susceptibility data for the upper 100 m of Hole 810C are summarized in Figure 23. There is a great deal of variability in the data in the upper 20 m of the hole which gradually decreases in amplitude to about 50 mbsf before increasing again. The magnetic susceptibility variations in the upper 10 m of Hole 810C can be used to determine the offset with Hole 810A (Fig. 24). The identification of the magnetic anomaly pattern and biostratigraphic determinations of age at Site 810 indicate that there is a possible hiatus in Core 132-810C-1H between the Brunhes and the Matuyama chrons. The Brunhes sequence is either a condensed section or is missing from this site; however, an expanded Matuyama and Gauss sequence is preserved. Continued refinements of the stratigraphic ages will help resolve the identification of this boundary (see "Paleomagnetism" section, this chapter).

Rapid, high-amplitude fluctuations in susceptibility are observed between 80–87 and 94–100 mbsf. The data over large

portions of the record exhibit an apparent cyclicity which is illustrated in Figure 25 for the interval between 14 and 30 mbsf. A series of high-amplitude susceptibility fluctuations beginning at 94.8 mbsf is followed by a significant drop in susceptibility at 99.5 mbsf near a probable hiatus (Fig. 26). A possible hiatus observed near 103.5 mbsf is reflected by a decrease in susceptibility (Fig. 27). A disturbed zone in the susceptibility record from 108 to 113 mbsf in Core 132-810C-13H, related to sedimentary slumping, precedes the transition to the early Maestrichtian.

GRAPE Bulk Density

Whole-core bulk density was measured using the GRAPE at Site 810. The closely spaced sampling intervals for magnetic susceptibility resulted in multiple density determinations at each discrete location along the core which had to be averaged to plot the data. The GRAPE data should prove a useful tool for analyzing lithologic variability downhole, for investigating proxy climatic signals recorded in the sediments, and for constructing an acoustic impedance record, when combined with the *p*-wave velocity data, to compare with the 3.5 kHz profile collected at this site. The amount of data collected and time constraints prevent the detailed analysis of this information in this report, however the raw data is displayed for 20 m intervals downhole in Figure 28. A long-wavelength sinusoidal pattern is observed in the bulk density data throughout the nannofossil ooze of Lithostratigraphic Units II and III.

The GRAPE data collected at Hole 810A are displayed in Figure 29. A plot of data from the upper 15 m of Hole 810C is shown in Figure 30. The sharp increase in density at about 0.7 mbsf may indicate the position of a hiatus in Core 132-810C-1H. As was the case with the susceptibility data, an offset of about 0.5–0.75 m can be observed in the GRAPE bulk density profile between Holes 810A and 810C.

P-wave Logger–Compressional Wave Velocity

Compressional wave velocity was measured at Site 810 using the PWL. The data were collected at a spacing of 2 cm and filtered to remove intervals having low signal strengths which represent noise. The velocities were generally in the range 1560–1620 m/s throughout the section, however there was much variability in the data. The data presented in Figure 31 in 20 m sections have not been corrected for *in-situ* temperature or pressure. Velocity peaks representing volcanic ash horizons are observed at 23.1 and 37.4 mbsf in Figure 31B; and at 47.8 mbsf in Figure 31C. The long-wavelength sinusoidal pattern observed in the GRAPE data can also be seen in the velocities, especially from 40 to 80 mbsf. In the lower part of the hole, sharp increases in velocity are associated with inferred hiatuses and interpreted changes in magnetic polarity at 69.5, 85.5, 96.6(?), and 99.5 mbsf, respectively. Data collected in the zone from 88.5 to 92.6 are anomalously low and may reflect a problem with the PWL transducer spacing. These data are not shown in Figure 31E because of their anomalous nature. Velocities decrease gradually from about 106 to 110 mbsf. This trend is also observed in bulk density through this zone. Below 110 mbsf the velocities increase again to the depth of the first recovered chert nodule at about 120 mbsf. Velocities measured by the PWL below the chert layer at 127.1 mbsf in Core 132-810C-16X range from 1620 to 1680 m/s.

Conclusion

The physical properties collected at Site 810 provide a wealth of information which can be used to interpret the local sedimentary history and help locate depositional or erosional hiatuses. Additionally, Milankovitch orbital periodicities in the flux of

Table 4. Torvane shear strength in kilopascals (kPa), measured perpendicular to bedding at the ends of whole-round core-sections at Site 810.

LEG	SITE	H	CORE	S	TOP	BOT	MBSF	kPa	TSE	KSF
132	810	C	1 H	1	150	150	1.5	7.8	.08	.04
132	810	C	2 H	2	0	0	3.9	13.7	.14	.07
132	810	C	2 H	3	0	0	5.4	13.3	.14	.07
132	810	C	2 H	4	150	150	8.4	15.7	.16	.08
132	810	C	3 H	1	150	150	13.4	25.5	.27	.13
132	810	C	3 H	3	150	150	16.4	11.8	.12	.06
132	810	C	3 H	6	150	150	20.9	19.6	.2	.1
132	810	C	4 H	1	150	150	22.9	27.5	.29	.14
132	810	C	4 H	4	150	150	27.4	23.5	.25	.12
132	810	C	4 H	6	150	150	30.4	23.5	.25	.12
132	810	C	5 H	1	150	150	32.4	28.4	.3	.15
132	810	C	5 H	3	150	150	35.4	30.4	.32	.16
132	810	C	5 H	6	150	150	39.9	23.5	.25	.12
132	810	C	6 H	1	150	150	41.9	41.2	.43	.22
132	810	C	6 H	4	150	150	46.4	55.9	.58	.29
132	810	C	6 H	5	150	150	47.9	49	.51	.26
132	810	C	7 H	1	150	150	51.4	27.5	.29	.14
132	810	C	7 H	3	150	150	54.4	46.1	.48	.24
132	810	C	7 H	5	150	150	57.4	62.8	.66	.33
132	810	C	8 H	3	0	0	62.4	53.9	.56	.28
132	810	C	8 H	5	0	0	65.4	54.9	.57	.29
132	810	C	8 H	6	150	150	68.4	46.1	.48	.24
132	810	C	9 H	2	0	0	70.4	52	.54	.27
132	810	C	9 H	3	150	150	73.4	57.9	.6	.3
132	810	C	9 H	5	0	0	74.9	68.6	.72	.36
132	810	C	10 H	2	150	150	81.4	43.1	.45	.23
132	810	C	10 H	5	0	0	84.4	44.1	.46	.23
132	810	C	10 H	6	150	150	87.4	56.9	.59	.3
132	810	C	11 H	1	150	150	89.4	48.1	.5	.25
132	810	C	11 H	3	150	150	92.4	37.3	.39	.19
132	810	C	11 H	5	150	150	95.4	45.1	.47	.24
132	810	C	11 H	7	0	0	96.9	29.4	.31	.15
132	810	C	12 H	2	0	0	98.9	52	.54	.27
132	810	C	13 H	4	150	150	112.9	13.7	.14	.07
132	810	C	13 H	6	150	150	115.9	19.6	.2	.1

aeolian materials to this site can be investigated using this data. The fine-scale lithologic variability observed in the magnetic susceptibility, bulk density, and velocity data and high sedimentation rates found throughout the Pliocene should provide the opportunity to investigate the paleoclimatic record preserved at this site. The Pliocene record is particularly important because an order of magnitude increase in the dust flux from continents to the North Pacific occurred during this time period (Rea and Leinen, 1988) reflecting changes in atmospheric and oceanic circulation in the northern hemisphere.

REFERENCES

- Bryant, W. B., Bennett, R. H., and Katherman, C. E., 1981. Shear strength, consolidation, porosity, and permeability of oceanic sediments. In Emiliani, C. (Ed.), *The Sea* (Vol. 7): New York (Wiley), 1555-1616.
- Ekdale, A. A., Bromley, R. G., and Pemberton, S. G., 1984. *Ichnology, the Use of Trace Fossils in Sedimentology and Stratigraphy*: Tulsa, OK (Soc. Econ. Paleontol. Mineral.).
- Fischer, A. G., Heezen, B. C., et al., 1971. *Init. Repts. DSDP*, 6: Washington (U.S. Govt. Printing Office).
- Heath, G. R., Burckle, L. H., et al., 1985. *Init. Repts. DSDP*, 86: Washington (U.S. Govt. Printing Office).
- Hovan, S. A., Rea, D. K., Pisias, N. G., and Shackleton, N. J., 1989. A direct link between the China loess and marine $\delta^{18}\text{O}$ records: aeolian flux to the North Pacific. *Nature*, 340:296-298.
- Janecek, T. R., and Rea, D. K., 1984. Pleistocene fluctuations in Northern Hemisphere tradewinds and westerlies. In Berger, A. L., Imbrie, J., Hayse, J., Kukla, G., and Saltzman, B. (Eds.), *Milankovitch and Climate* (Pt. 1): Dordrecht (D. Reidel), 331-347.
- Kenter, J.A.M., and Schlager, W., 1989. A comparison of shear strength in calcareous and siliciclastic marine sediments. *Mar. Geol.*, 88:145-152.

Kukla, G., Heller, F., Ming, L. X., Chun, X. T., Sheng, L. T., and Sheng, A. Z., 1988. Pleistocene climates in China dated by magnetic susceptibility. *Geology*, 16:811-814.

Larson, R. L., Moberly, R., et al., 1975. *Init. Repts. DSDP*, 32: Washington (U.S. Govt. Printing Office).

Lee, H. J., 1982. Bulk density and shear strength of several deep-sea calcareous sediments. In Demars, K. R., and Chaney, R. C. (Eds.), *Geotechnical Properties, Behavior, and Performance of Calcareous Soils*. ASTM Spec. Tech. Publ. 777:54-78.

Luterbacher, H. P., 1975. Paleocene and early Eocene planktonic foraminifera Leg 32, Deep Sea Drilling Project. In Larson, R. L., Moberly, R., et al., *Init. Repts. DSDP*, 32: Washington (U.S. Govt. Printing Office), 725-733.

Pisias, N. G., and Leinen, M., 1984. Milankovitch forcing of the oceanic system: evidence from the northwest Pacific. In Berger, A. L., Imbrie, J., Hayse, J., Kukla, G., and Saltzman, B. (Eds.), *Milankovitch and Climate* (Pt. 1): Dordrecht (D. Reidel), 307-330.

Rea, D. K., and Janecek, T. R., 1981. Mass accumulation rates of the non-authigenic, inorganic, crystalline (eolian) component of deep-sea sediments from the western mid-Pacific Mountains, DSDP Site 463. In Theide, J., Vallier, T. L., et al. *Init. Repts. DSDP*, 62: Washington (U.S. Govt. Printing Office), 653-659.

Rea, D. K., and Leinen, M., 1988. Asian aridity and the zonal westerlies: late Pleistocene and Holocene record of eolian deposition in the Northwest Pacific Ocean. *Palaeogeogr., Palaeoclimatol., Palaeoecol.*, 66:1-8.

Schlanger, S. O., and Jenkyns, H. C., 1976. Cretaceous oceanic anoxic events: causes and consequences. *Geol. Mijnbouw*, 55:179-184.

Vincent, E., 1975. Neogene planktonic foraminifera from the Central North Pacific, Leg 32, Deep Sea Drilling Project. In Larson, R. L., Moberly, R., et al., *Init. Repts. DSDP*, 32: Washington (U.S. Govt. Printing Office), 765-801.

Ms 132-104

NOTE: All core description forms ("barrel sheets") and core photographs have been printed on coated paper and bound as Section 4, near the back of the book, beginning on page 241.

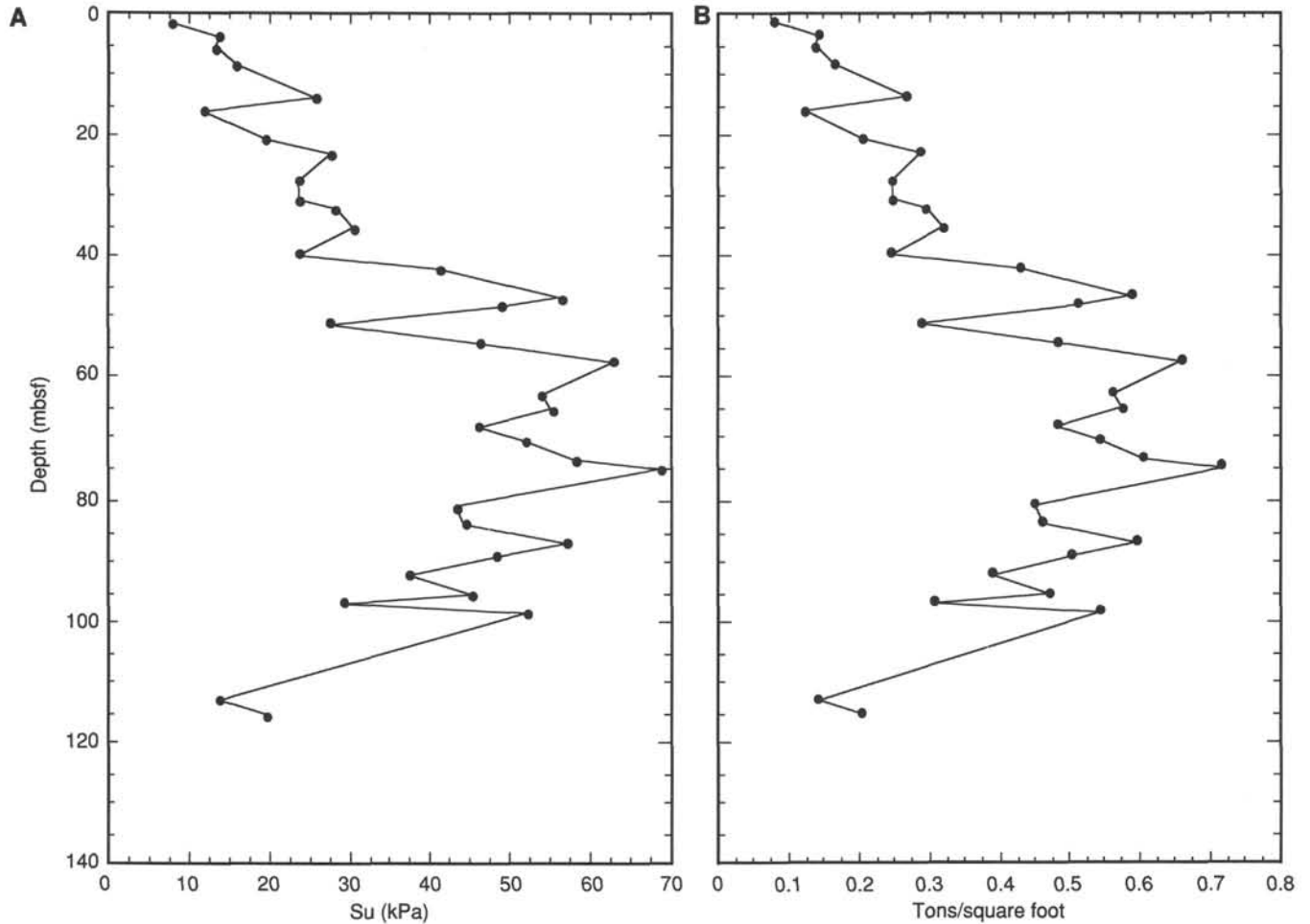


Figure 19. Plot of vane shear strength (Su) vs. depth (mbsf) for Site 810. **A.** Shear strength in kilopascals (kPa) measured with the hand-held Torvane perpendicular to bedding on the whole-round cores. **B.** Shear strength in tons/square foot (TSF) measured as in A.

Table 5. Vane shear strengths (kPa) measured on the working-half of split-core sections, parallel to bedding, using the Wykeham-Farrance motorized vane device at Site 810.

<u>LEG</u>	<u>SITE</u>	<u>H</u>	<u>CORE</u>		<u>S</u>	<u>TOP</u>	<u>BOT</u>	<u>MBSF</u>	<u>kPa</u>
132	810	C	1	H	1	130	131	1.3	71
132	810	C	1	H	2	25	26	1.75	14
132	810	C	2	H	1	109	110	3.49	18
132	810	C	2	H	3	69	70	6.09	26
132	810	C	2	H	5	77	78	9.17	38
132	810	C	3	H	3	131	132	16.21	52
132	810	C	3	H	5	89	90	18.79	62
132	810	C	3	H	7	16	17	21.06	121
132	810	C	4	H	2	69	70	23.59	23
132	810	C	4	H	4	57	59	26.47	18
132	810	C	4	H	6	127	128	30.17	35
132	810	C	5	H	1	76	77	31.66	24
132	810	C	5	H	4	116	117	36.56	22
132	810	C	5	H	6	129	130	39.69	36
132	810	C	6	H	2	91	92	42.81	34
132	810	C	6	H	4	124	125	46.14	53
132	810	C	7	H	1	64	66	50.54	48
132	810	C	7	H	5	125	127	57.15	100
132	810	C	8	H	2	125	127	62.15	54
132	810	C	8	H	6	123	125	68.13	56
132	810	C	9	H	1	67	69	69.57	96
132	810	C	9	H	6	107	109	77.47	50
132	810	C	10	H	3	116	118	82.56	37
132	810	C	10	H	6	114	116	87.04	59
132	810	C	11	H	2	133	135	90.73	20
132	810	C	11	H	7	14	16	97.04	95
132	810	C	12	H	1	133	135	98.73	26
132	810	C	12	H	6	102	104	105.92	18
132	810	C	13	H	5	110	112	114	20
132	810	C	14	H	1	128	130	117.68	22
132	810	C	14	H	6	65	67	124.55	21

Table 6. Gravimetric determinations of density made at Site 810.

LEG	SITE	H	C	I	S	TOP	MBSF	WBD	DBD	GD
132	810	C	1	H	1	8	.08	1.55	.74	2.80
132	810	C	1	H	1	78	.78	1.59	.83	2.77
132	810	C	1	H	1	130	1.30	1.58	.83	2.73
132	810	C	1	H	2	25	1.75	1.50	.72	2.65
132	810	C	2	H	1	39	2.79	1.43	.79	2.67
132	810	C	2	H	1	69	3.09	1.63	.91	2.72
132	810	C	2	H	1	109	3.49	1.53	.75	2.83
132	810	C	2	H	2	13	4.03	1.61	.85	3.27
132	810	C	2	H	2	69	4.59	1.64	.90	2.78
132	810	C	2	H	2	119	5.09	1.64	.89	2.78
132	810	C	2	H	3	29	5.69	1.52	.73	2.79
132	810	C	2	H	3	69	6.09	1.59	.86	2.77
132	810	C	2	H	3	109	6.49	1.61	.89	2.70
132	810	C	2	H	4	9	6.99	1.59	.86	2.69
132	810	C	2	H	4	69	7.59	1.63	.91	2.77
132	810	C	2	H	4	109	7.99	1.61	.89	2.81
132	810	C	2	H	5	29	8.69	1.56	.83	2.77
132	810	C	2	H	5	78	9.18	1.62	.89	2.71
132	810	C	2	H	5	139	9.79	1.68	.97	2.67
132	810	C	2	H	6	29	10.19	1.55	.78	2.76
132	810	C	2	H	6	69	10.59	1.55	.79	2.78
132	810	C	2	H	6	129	11.19	1.62	.91	2.79
132	810	C	2	H	7	29	11.69	1.62	.86	2.66
132	810	C	3	H	1	40	12.3	1.68	.89	2.8
132	810	C	3	H	1	140	13.3	1.59	.86	2.73
132	810	C	3	H	2	60	14.00	1.63	.93	2.75
132	810	C	3	H	2	100	14.40	1.64	.93	2.82
132	810	C	3	H	2	140	14.8	1.64	.92	2.79
132	810	C	3	H	3	19	15.09	1.63	.92	2.78
132	810	C	3	H	3	69	15.59	1.61	.9	2.66
132	810	C	3	H	3	130	16.2	1.61	.87	2.77
132	810	C	3	H	4	19	16.59	1.62	.87	2.83
132	810	C	3	H	4	69	17.09	1.6	.88	2.69
132	810	C	3	H	4	130	17.7	1.6	.87	2.73
132	810	C	3	H	5	19	18.09	1.64	.94	2.67
132	810	C	3	H	5	89	18.79	1.64	.92	2.74
132	810	C	3	H	5	130	19.2	1.62	.89	2.55
132	810	C	3	H	6	9	19.49	1.66	.94	2.78
132	810	C	3	H	6	60	20	1.6	.87	2.77
132	810	C	3	H	6	100	20.4	1.64	.94	2.74
132	810	C	3	H	6	140	20.8	1.73	1.08	2.72
132	810	C	3	H	7	16	21.06	1.69	1.01	2.77
132	810	C	3	H	7	60	21.5	1.7	1.01	2.78
132	810	C	4	H	1	19	21.59	1.59	.84	2.81
132	810	C	4	H	1	50	21.9	1.65	.95	2.76
132	810	C	4	H	1	86	22.26	1.67	.99	2.74
132	810	C	4	H	1	140	22.8	1.64	.92	2.77
132	810	C	4	H	2	40	23.3	1.69	1.01	2.71
132	810	C	4	H	2	70	23.6	1.65	.94	2.77
132	810	C	4	H	2	140	24.3	1.66	.98	2.71
132	810	C	4	H	3	20	24.6	1.61	.89	2.71

Table 6 (continued).

<u>LEG</u>	<u>SITE</u>	<u>H</u>	<u>C</u>	<u>I</u>	<u>S</u>	<u>TOP</u>	<u>MBSF</u>	<u>WBD</u>	<u>DBD</u>	<u>GD</u>
132	810	C	4	H	3	70	25.1	1.63	.92	2.8
132	810	C	4	H	3	120	25.6	1.64	.94	2.69
132	810	C	4	H	4	20	26.1	1.65	.96	2.76
132	810	C	4	H	4	57	26.47	1.59	.86	2.69
132	810	C	4	H	4	120	27.1	1.63	.94	2.71
132	810	C	4	H	5	9	27.49	1.63	.91	2.76
132	810	C	4	H	5	38	27.78	1.57	.81	2.69
132	810	C	4	H	5	70	28.1	1.58	.85	2.67
132	810	C	4	H	5	119	28.59	1.61	.88	2.78
132	810	C	4	H	6	20	29.1	1.63	.93	2.72
132	810	C	4	H	6	70	29.6	1.67	.99	2.72
132	810	C	4	H	6	127	30.17	1.65	.95	2.77
132	810	C	4	H	7	20	30.6	1.68	.98	2.8
132	810	C	4	H	7	60	31	1.64	.94	2.74
132	810	C	5	H	1	19	31.09	1.71	1.05	2.77
132	810	C	5	H	1	76	31.66	1.59	.9	2.73
132	810	C	5	H	1	130	32.2	1.58	.9	2.76
132	810	C	5	H	2	20	32.6	1.7	1.04	2.76
132	810	C	5	H	2	70	33.1	1.68	.99	2.73
132	810	C	5	H	2	130	33.7	1.67	.99	2.74
132	810	C	5	H	3	20	34.1	1.65	.97	2.64
132	810	C	5	H	3	70	34.6	1.65	.95	2.72
132	810	C	5	H	3	130	35.2	1.63	.9	2.74
132	810	C	5	H	4	39	35.79	1.64	.91	2.76
132	810	C	5	H	4	115	36.55	1.63	.92	2.78
132	810	C	5	H	5	20	37.1	1.69	1.02	2.72
132	810	C	5	H	5	64	37.54	1.67	1.07	2.46
132	810	C	5	H	5	116	38.06	1.63	.91	2.75
132	810	C	5	H	6	20	38.6	1.69	.99	2.8
132	810	C	5	H	6	70	39.1	1.7	1.02	2.8
132	810	C	5	H	6	130	39.7	1.61	.9	2.7
132	810	C	5	H	7	20	40.1	1.61	.91	2.7
132	810	C	5	H	7	40	40.3	1.59	.83	2.77
132	810	C	6	H	1	39	40.79	1.71	1.04	2.83
132	810	C	6	H	1	120	41.6	1.7	1.05	2.72
132	810	C	6	H	2	40	42.3	1.69	1.02	2.76
132	810	C	6	H	2	90	42.8	1.71	1.03	2.81
132	810	C	6	H	3	40	43.8	1.73	1.06	2.82
132	810	C	6	H	3	120	44.6	1.68	1.01	2.75
132	810	C	6	H	4	40	45.3	1.68	1	2.76
132	810	C	6	H	4	123	46.13	1.67	.97	2.75
132	810	C	6	H	5	40	46.8	1.66	.99	2.84
132	810	C	6	H	5	120	47.6	1.64	.92	2.79
132	810	C	6	H	6	29	48.19	1.34	.43	2.79
132	810	C	6	H	6	120	49.1	1.7	1.03	2.74
132	810	C	6	H	7	40	49.8	1.7	1.03	2.75
132	810	C	7	H	1	20	50.1	1.67	1	2.78
132	810	C	7	H	1	64	50.54	1.63	.94	2.77
132	810	C	7	H	1	130	51.2	1.71	1.04	2.84
132	810	C	7	H	2	20	51.6	1.73	1.05	2.67

Table 6 (continued).

<u>LEG</u>	<u>SITE</u>	<u>H</u>	<u>C</u>	<u>I</u>	<u>S</u>	<u>TOP</u>	<u>MBSE</u>	<u>WBD</u>	<u>DBD</u>	<u>GD</u>
132	810	C	7	H	2	130	52.7	1.68	1.01	2.77
132	810	C	7	H	3	20	53.1	1.69	1.01	2.82
132	810	C	7	H	3	130	54.2	1.7	1.04	2.81
132	810	C	7	H	4	20	54.6	1.71	1.04	2.81
132	810	C	7	H	4	110	55.5	1.69	1.01	2.69
132	810	C	7	H	5	20	56.1	1.73	1.05	2.74
132	810	C	7	H	5	79	56.69	1.62	.89	2.78
132	810	C	7	H	5	125	57.15	1.64	.93	2.83
132	810	C	7	H	6	20	57.6	1.68	.99	2.85
132	810	C	7	H	6	130	58.7	1.65	.93	2.72
132	810	C	7	H	7	20	59.1	1.71	1.01	2.79
132	810	C	8	H	1	59	59.99	1.65	.94	2.75
132	810	C	8	H	1	130	60.7	1.64	.92	2.71
132	810	C	8	H	2	60	61.5	1.69	1	2.71
132	810	C	8	H	2	125	62.15	1.68	.99	2.71
132	810	C	8	H	3	60	63	1.69	.97	2.83
132	810	C	8	H	4	60	64.5	1.71	1.03	2.75
132	810	C	8	H	5	60	66	1.7	1.04	2.7
132	810	C	8	H	6	60	67.5	1.98	1.14	5.11
132	810	C	8	H	6	123	68.13	1.65	.94	2.8
132	810	C	8	H	7	60	69	1.66	.94	2.73
132	810	C	9	H	1	67	69.57	1.61	.86	2.84
132	810	C	9	H	2	68	71.08	1.69	1.03	2.73
132	810	C	9	H	3	69	72.59	1.73	1.08	2.75
132	810	C	9	H	4	68	74.08	1.75	1.06	2.87
132	810	C	9	H	5	28	75.18	1.69	1	2.79
132	810	C	9	H	5	119	76.09	1.68	.98	2.77
132	810	C	9	H	6	19	76.59	1.6	.88	2.65
132	810	C	9	H	6	107	77.47	1.65	.93	2.8
132	810	C	9	H	7	19	78.09	1.72	1.03	2.82
132	810	C	10	H	1	116	79.56	1.67	.96	2.84
132	810	C	10	H	2	117	81.07	1.66	.97	2.71
132	810	C	10	H	3	116	82.56	1.64	.93	2.74
132	810	C	10	H	4	116	84.06	1.71	1.03	2.8
132	810	C	10	H	5	117	85.57	1.71	1.04	2.8
132	810	C	10	H	6	35	86.25	1.64	.95	2.71
132	810	C	10	H	6	113	87.03	1.71	1.03	2.83
132	810	C	10	H	7	58	87.98	1.71	1.05	2.76
132	810	C	11	H	1	39	88.29	1.71	1.05	2.73
132	810	C	11	H	1	132	89.22	1.73	1.07	2.69
132	810	C	11	H	2	133	90.73	1.77	1.12	2.73
132	810	C	11	H	3	133	92.23	1.69	1	2.69
132	810	C	11	H	4	134	93.74	1.73	1.06	2.71
132	810	C	11	H	6	38	95.78	1.74	1.08	2.73
132	810	C	11	H	7	14	97.04	1.74	1.1	2.68
132	810	C	11	H	7	60	97.5	1.76	1.11	2.7
132	810	C	12	H	1	30	97.7	1.7	1.03	2.76
132	810	C	12	H	1	133	98.73	1.7	1.02	2.7
132	810	C	12	H	2	134	100.24	1.86	1.3	2.71
132	810	C	12	H	3	134	101.74	1.86	1.3	2.73

Table 6 (continued).

<u>LEG</u>	<u>SITE</u>	<u>H</u>	<u>C</u>	<u>I</u>	<u>S</u>	<u>TOP</u>	<u>MBSF</u>	<u>WBD</u>	<u>DBD</u>	<u>GD</u>
132	810	C	12	H	5	40	103.8	1.88	1.38	2.88
132	810	C	12	H	6	102	105.92	1.88	1.32	2.79
132	810	C	13	H	1	90	107.8	1.84	1.27	2.73
132	810	C	13	H	2	90	109.3	1.77	1.16	2.76
132	810	C	13	H	2	120	109.6	1.74	1.1	2.77
132	810	C	13	H	3	130	111.2	1.81	1.19	2.77
132	810	C	13	H	4	90	112.3	1.77	1.15	2.76
132	810	C	13	H	5	35	113.25	1.83	1.25	2.72
132	810	C	13	H	5	110	114	1.81	1.2	2.75
132	810	C	13	H	6	59	114.99	1.77	1.15	2.79
132	810	C	14	H	1	128	117.68	1.73	1.08	2.84
132	810	C	14	H	2	79	118.69	1.7	1.05	2.74
132	810	C	14	H	3	65	120.05	1.83	1.25	2.81
132	810	C	14	H	3	88	120.28	2.65	2.6	2.94
132	810	C	14	H	5	116	123.56	1.75	1.14	2.78
132	810	C	14	H	6	35	124.25	1.76	1.13	2.74
132	810	C	14	H	6	99	124.89	1.83	1.21	2.81
132	810	C	15	H	1	50	126.4	1.76	1.13	2.76
132	810	C	15	H	1	100	126.9	1.78	1.18	2.79
132	810	C	15	H	2	100	128.4	1.69	.98	2.8
132	810	C	15	H	4	35	130.75	1.59	.85	2.73
132	810	C	15	H	5	20	132.1	1.56	.8	2.76
132	810	C	16	X	1	1	127.11	2.67	2.61	2.63
132	810	C	16	X	1	131	128.41	1.83	1.07	2.84
132	810	C	16	X	2	97	129.57	1.76	1.13	2.79

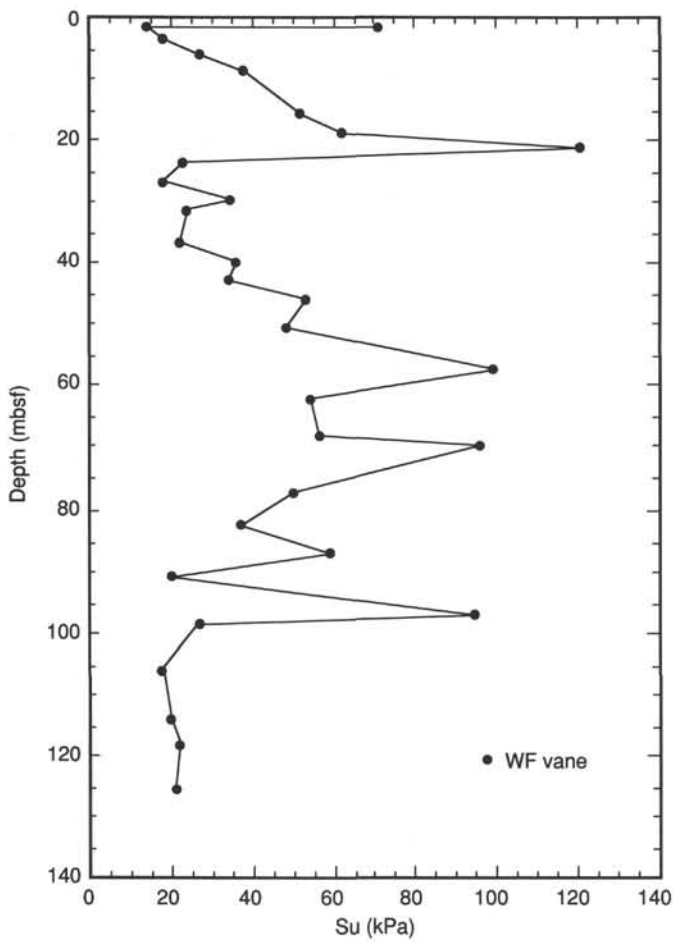


Figure 20. Plot of vane shear strength (Su) vs. depth (mbsf) for Site 810. Vane shear strength in kPa measured with the Wykeham-Farrance motorized shear device parallel to bedding on the working-half of the split-cores.

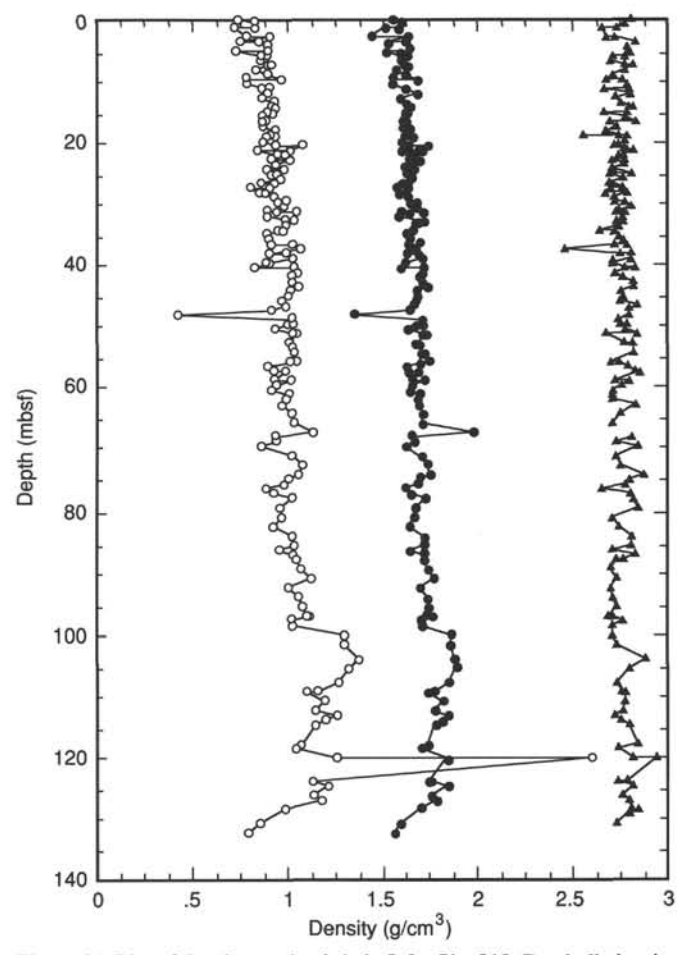


Figure 21. Plot of density vs. depth (mbsf) for Site 810. Dry-bulk density (open circles), wet-bulk density (solid circles), and grain density (solid triangles) in g/cm³, respectively.

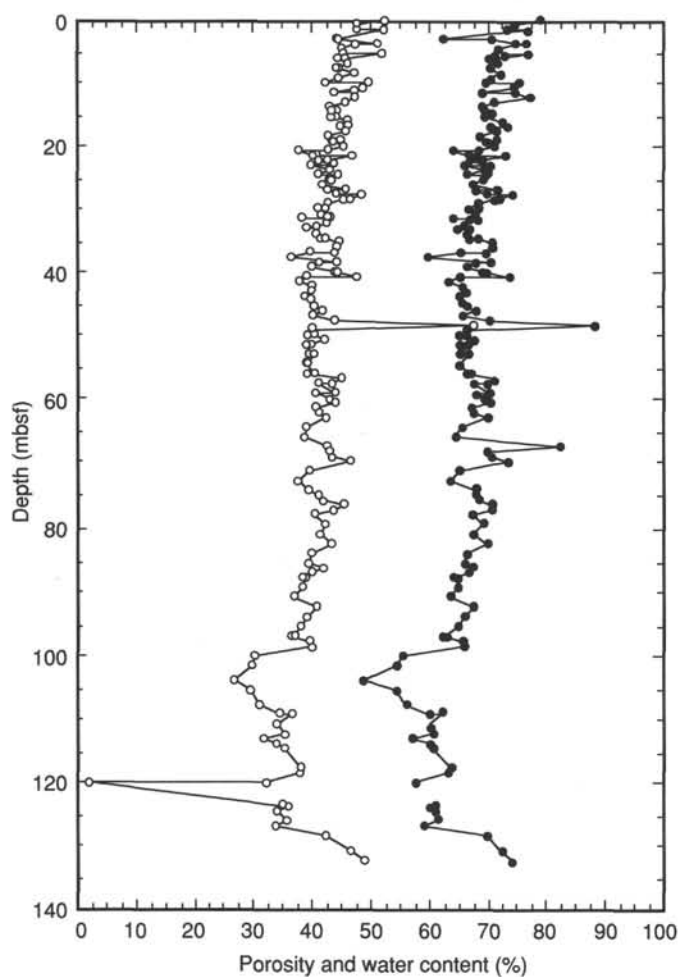


Figure 22. Plot of porosity (solid circles) and water content (open circles = %wet-sample weight) in percent vs. depth (mbsf) for Site 810.

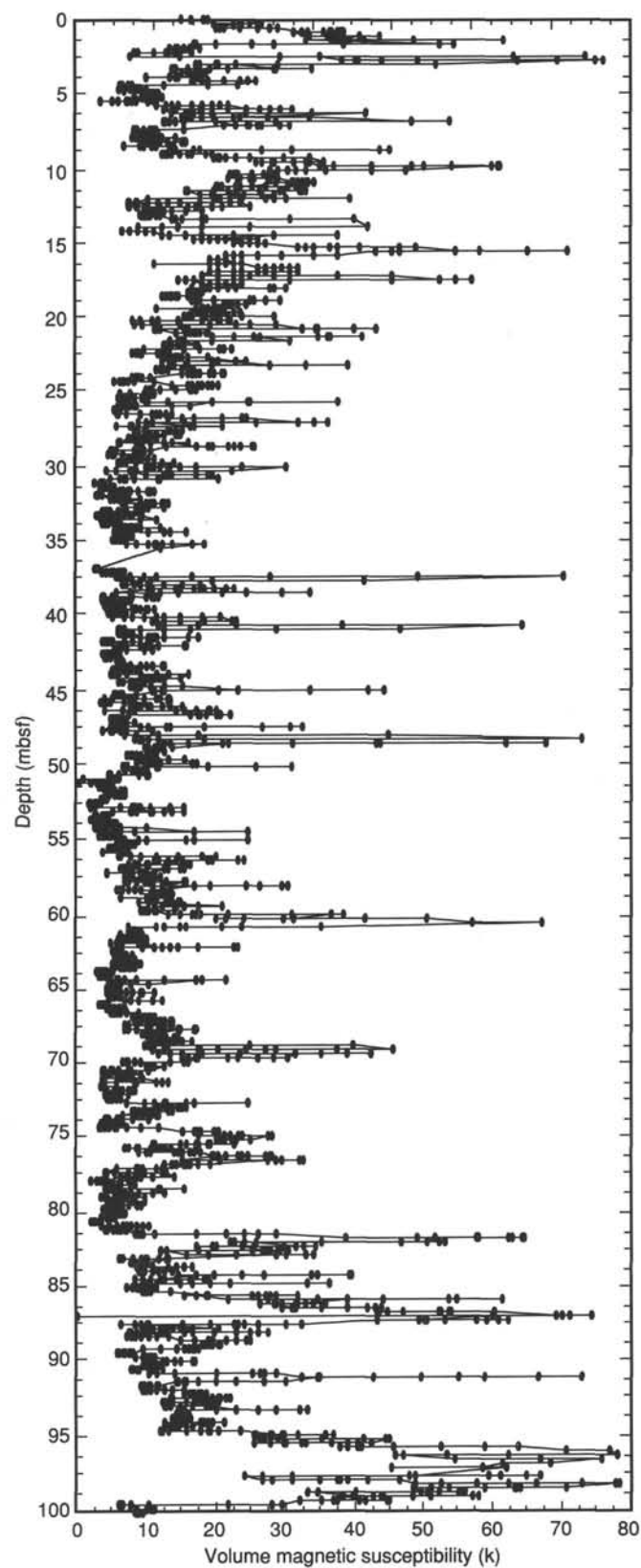


Figure 23. Plot of volume magnetic susceptibility (k) vs. depth from the mud line to 100 mbsf for Hole 810C.

Table 7. Gravimetric determinations of porosity and water content made at Site 810.

LEG	SITE	H	CORE	S	TOP	MBSF	POR1	POR2	WC/W	WC/D	VR1	VR2	
132	810	C	1	H	1	8	.08	79.2	75.3	52.4	110	3.8	3.01
132	810	C	1	H	1	78	.78	74.3	71.4	47.7	91.3	2.89	2.46
132	810	C	1	H	1	130	1.3	73.4	71.1	47.6	91	2.76	2.42
132	810	C	1	H	2	25	1.75	76.7	74.2	52.3	109.6	3.29	2.83
132	810	C	2	H	1	39	2.79	62.2	68.1	44.6	80.6	1.65	2.1
132	810	C	2	H	1	69	3.09	70.6	68.2	44.3	79.5	2.4	2.11
132	810	C	2	H	1	109	3.49	76.5	74.7	51.2	104.9	3.25	2.9
132	810	C	2	H	2	13	4.03	74.3	74.3	47.3	89.7	2.9	2.86
132	810	C	2	H	2	69	4.59	71.7	69.1	44.8	81.2	2.53	2.2
132	810	C	2	H	2	119	5.09	72.8	69.7	45.5	83.5	2.68	2.27
132	810	C	2	H	3	29	5.69	76.9	74.9	52	108.2	3.33	2.95
132	810	C	2	H	3	69	6.09	70.8	69.7	45.6	84	2.42	2.27
132	810	C	2	H	3	109	6.49	70.3	68.4	44.7	80.8	2.37	2.13
132	810	C	2	H	4	9	6.99	71.5	69.4	46	85.2	2.51	2.24
132	810	C	2	H	4	69	7.59	70	68.4	44.1	78.9	2.33	2.13
132	810	C	2	H	4	109	7.99	70.3	69.1	44.6	80.6	2.37	2.21
132	810	C	2	H	5	29	8.69	71.9	71	47.1	89.2	2.55	2.41
132	810	C	2	H	5	78	9.18	70.4	68.4	44.6	80.6	2.38	2.13
132	810	C	2	H	5	139	9.79	69.3	65.8	42.2	73.1	2.25	1.9
132	810	C	2	H	6	29	10.19	75.2	73.1	49.8	99.3	3.03	2.68
132	810	C	2	H	6	69	10.59	74.3	72.6	49	96.2	2.9	2.61
132	810	C	2	H	6	129	11.19	69.1	68.2	43.7	77.6	2.23	2.12
132	810	C	2	H	7	29	11.69	74.5	70.1	47.1	89	2.92	2.31
132	810	C	3	H	1	40	12.3	77.3	71.1	47.1	89	3.4	2.43
132	810	C	3	H	1	140	13.3	71.1	69.6	45.9	84.8	2.46	2.26
132	810	C	3	H	2	60	14	69	67.5	43.2	76.2	2.22	2.05
132	810	C	3	H	2	100	14.4	69.5	68	43.3	76.3	2.27	2.1
132	810	C	3	H	2	140	14.8	70.4	68.4	44	78.5	2.38	2.14
132	810	C	3	H	3	19	15.09	69.4	68	43.6	77.4	2.27	2.1
132	810	C	3	H	3	69	15.59	69.5	67.6	44.2	79.2	2.28	2.06
132	810	C	3	H	3	130	16.2	72.3	70.1	46.1	85.5	2.61	2.31
132	810	C	3	H	4	19	16.59	73.3	70.7	46.3	86.1	2.75	2.38
132	810	C	3	H	4	69	17.09	70.6	68.6	45.1	82.1	2.4	2.15
132	810	C	3	H	4	130	17.7	71.2	69.4	45.6	83.8	2.47	2.23
132	810	C	3	H	5	19	18.09	68.6	66.4	42.8	74.7	2.18	1.95
132	810	C	3	H	5	89	18.79	69.9	67.8	43.8	77.8	2.32	2.08
132	810	C	3	H	5	130	19.2	71.2	67.4	45	81.7	2.47	2.04
132	810	C	3	H	6	9	19.49	70.3	67.9	43.4	76.7	2.36	2.08
132	810	C	3	H	6	60	20	71	69.5	45.4	83.3	2.45	2.25
132	810	C	3	H	6	100	20.4	68.1	66.7	42.5	73.9	2.13	1.97
132	810	C	3	H	6	140	20.8	63.8	61.9	37.7	60.5	1.76	1.61
132	810	C	3	H	7	16	21.06	66.8	65	40.4	67.7	2.01	1.83
132	810	C	3	H	7	60	21.5	67.5	65.3	40.7	68.6	2.08	1.86
132	810	C	4	H	1	19	21.59	73	71.1	47	88.6	2.7	2.42
132	810	C	4	H	1	50	21.9	68.8	66.9	42.6	74.2	2.21	2
132	810	C	4	H	1	86	22.26	66.8	65.2	41	69.4	2.01	1.85
132	810	C	4	H	1	140	22.8	70.2	68.2	43.9	78.4	2.36	2.12
132	810	C	4	H	2	40	23.3	65.9	64.1	40	66.6	1.93	1.76
132	810	C	4	H	2	70	23.6	69.4	67.5	43.2	75.9	2.27	2.05
132	810	C	4	H	2	140	24.3	66.3	65.1	41.1	69.7	1.97	1.84
132	810	C	4	H	3	20	24.6	69.6	68.1	44.4	79.8	2.29	2.11
132	810	C	4	H	3	70	25.1	69.3	68.2	43.6	77.3	2.26	2.11
132	810	C	4	H	3	120	25.6	68.8	66.7	43	75.4	2.21	1.98
132	810	C	4	H	4	20	26.1	67.6	66.4	42	72.3	2.09	1.95
132	810	C	4	H	4	57	26.47	71.4	69.4	45.9	84.9	2.5	2.23

Table 7 (continued).

LEG	SITE	H	CORE	S	TOP	MBSF	POR1	POR2	WC/W	WC/D	VR1	VR2
132	810	C	4 H	4	120	27.1	67.7	66.4	42.5	73.8	2.1	1.95
132	810	C	4 H	5	9	27.49	69.9	68.2	44	78.5	2.32	2.12
132	810	C	4 H	5	38	27.78	74.1	71.5	48.5	94.1	2.87	2.47
132	810	C	4 H	5	70	28.1	71.6	69.7	46.5	86.8	2.52	2.27
132	810	C	4 H	5	119	28.59	71.1	69.4	45.2	82.5	2.46	2.24
132	810	C	4 H	6	20	29.1	68.3	66.8	42.8	74.9	2.15	1.99
132	810	C	4 H	6	70	29.6	66.8	65.1	40.9	69.3	2.01	1.84
132	810	C	4 H	6	127	30.17	68.1	66.6	42.2	73.1	2.14	1.97
132	810	C	4 H	7	20	30.6	67.9	66.2	41.5	71	2.12	1.94
132	810	C	4 H	7	60	31	68.2	66.7	42.5	74	2.15	1.98
132	810	C	5 H	1	19	31.09	63.8	62.9	38.3	62.1	1.76	1.68
132	810	C	5 H	1	76	31.66	66.6	67.1	43	75.5	1.99	2.01
132	810	C	5 H	1	130	32.2	65.8	67.1	42.8	74.8	1.92	2.01
132	810	C	5 H	2	20	32.6	64.9	63.5	39	64	1.85	1.72
132	810	C	5 H	2	70	33.1	66.8	65	40.8	68.8	2.01	1.84
132	810	C	5 H	2	130	33.7	66.1	64.9	40.6	68.3	1.95	1.83
132	810	C	5 H	3	20	34.1	66.8	64.9	41.4	70.7	2.01	1.82
132	810	C	5 H	3	70	34.6	68.1	66.4	42.4	73.6	2.14	1.95
132	810	C	5 H	3	130	35.2	70.5	68.5	44.4	79.9	2.39	2.14
132	810	C	5 H	4	39	35.79	70.7	68.4	44.2	79.2	2.41	2.14
132	810	C	5 H	4	115	36.55	69.5	68.1	43.7	77.5	2.28	2.1
132	810	C	5 H	5	20	37.1	65.3	63.9	39.7	65.8	1.88	1.75
132	810	C	5 H	5	64	37.54	59.4	58.1	36.4	57.1	1.46	1.37
132	810	C	5 H	5	116	38.06	70.1	68.2	44.1	78.9	2.34	2.12
132	810	C	5 H	6	20	38.6	67.7	65.8	41.1	69.7	2.09	1.9
132	810	C	5 H	6	70	39.1	66.2	64.8	40	66.6	1.96	1.82
132	810	C	5 H	6	130	39.7	69.3	67.8	44.1	78.8	2.26	2.08
132	810	C	5 H	7	20	40.1	68.8	67.5	43.8	77.8	2.21	2.05
132	810	C	5 H	7	40	40.3	73.8	71.3	47.5	90.6	2.81	2.45
132	810	C	6 H	1	39	40.79	65.3	64.2	39.1	64.2	1.88	1.77
132	810	C	6 H	1	120	41.6	63.3	62.3	38.1	61.5	1.73	1.63
132	810	C	6 H	2	40	42.3	65.6	64.3	39.8	66.1	1.91	1.78
132	810	C	6 H	2	90	42.8	66.4	64.7	39.8	66.2	1.98	1.81
132	810	C	6 H	3	40	43.8	65.2	63.6	38.6	62.9	1.87	1.73
132	810	C	6 H	3	120	44.6	65.5	64.3	39.9	66.3	1.9	1.78
132	810	C	6 H	4	40	45.3	66.4	65	40.5	68.1	1.97	1.84
132	810	C	6 H	4	123	46.13	68	66.1	41.8	71.8	2.12	1.93
132	810	C	6 H	5	40	46.8	65.5	65.5	40.4	67.8	1.9	1.88
132	810	C	6 H	5	120	47.6	70.3	68.3	43.9	78.3	2.37	2.13
132	810	C	6 H	6	29	48.19	88.3	85.3	67.6	208.2	7.52	5.67
132	810	C	6 H	6	120	49.1	66.2	64.1	39.8	66	1.96	1.76
132	810	C	6 H	7	40	49.8	65.3	63.7	39.3	64.8	1.88	1.74
132	810	C	7 H	1	20	50.1	66.2	65.2	40.5	68.1	1.96	1.85
132	810	C	7 H	1	64	50.54	67.4	66.7	42.2	73.1	2.06	1.98
132	810	C	7 H	1	130	51.2	65.2	64.2	39	64.1	1.87	1.77
132	810	C	7 H	2	20	51.6	66.7	63.2	39.4	65	2	1.7
132	810	C	7 H	2	130	52.7	65	64.3	39.7	65.9	1.86	1.78
132	810	C	7 H	3	20	53.1	66.8	65.4	40.4	67.8	2.01	1.87
132	810	C	7 H	3	130	54.2	65.1	64.1	39.1	64.3	1.87	1.76
132	810	C	7 H	4	20	54.6	65.1	63.9	39	63.8	1.86	1.75
132	810	C	7 H	4	110	55.5	66.6	64.3	40.4	67.7	2	1.78
132	810	C	7 H	5	20	56.1	66.3	63.6	39.3	64.6	1.96	1.73
132	810	C	7 H	5	79	56.69	71.1	69.2	45	81.7	2.46	2.22
132	810	C	7 H	5	125	57.15	69.7	68.3	43.5	76.9	2.3	2.13

Table 7 (continued).

LEG	SITE	H	CORE	S	TOP	MBSF	POR1	POR2	WC/W	WC/D	VR1	VR2
132	810	C	7 H	6	20	57.6	67.4	66.2	41.1	69.7	2.07	1.93
132	810	C	7 H	6	130	58.7	70.2	67.6	43.7	77.6	2.36	2.06
132	810	C	7 H	7	20	59.1	67.7	65.3	40.6	68.4	2.1	1.86
132	810	C	8 H	1	59	59.99	69.4	67.3	43.1	75.7	2.27	2.04
132	810	C	8 H	1	130	60.7	70.2	67.7	43.9	78.2	2.35	2.07
132	810	C	8 H	2	60	61.5	67.2	64.9	40.8	68.9	2.05	1.82
132	810	C	8 H	2	125	62.15	67.6	65.2	41.1	69.9	2.08	1.85
132	810	C	8 H	3	60	63	69.8	67.3	42.4	73.5	2.32	2.03
132	810	C	8 H	4	60	64.5	65.5	63.8	39.3	64.8	1.9	1.74
132	810	C	8 H	5	60	66	64.2	62.8	38.7	63.1	1.79	1.66
132	810	C	8 H	6	60	67.5	82.2	78.8	42.5	73.9	4.63	3.68
132	810	C	8 H	6	123	68.13	69.7	67.8	43.2	76.1	2.3	2.08
132	810	C	8 H	7	60	69	70.5	67.5	43.5	77	2.39	2.05
132	810	C	9 H	1	67	69.57	73.4	71.1	46.7	87.5	2.75	2.42
132	810	C	9 H	2	68	71.08	65.1	63.7	39.4	64.9	1.87	1.73
132	810	C	9 H	3	69	72.59	63.4	61.9	37.5	59.9	1.73	1.61
132	810	C	9 H	4	68	74.08	67.8	65.2	39.7	65.9	2.11	1.85
132	810	C	9 H	5	28	75.18	68	65.8	41.1	69.9	2.13	1.9
132	810	C	9 H	5	119	76.09	68.3	66.1	41.7	71.4	2.16	1.93
132	810	C	9 H	6	19	76.59	70.7	68.4	45.2	82.5	2.41	2.13
132	810	C	9 H	6	107	77.47	70.5	68.3	43.8	77.9	2.39	2.13
132	810	C	9 H	7	19	78.09	67.5	65.2	40.2	67.2	2.07	1.85
132	810	C	10H	1	116	79.56	68.8	67.3	42.3	73.2	2.2	2.03
132	810	C	10H	2	117	81.07	67.5	65.6	41.6	71.2	2.08	1.88
132	810	C	10H	3	116	82.56	69.6	67.5	43.5	76.9	2.29	2.05
132	810	C	10H	4	116	84.06	66.3	64.6	39.8	66.2	1.97	1.81
132	810	C	10H	5	117	85.57	65.9	64.3	39.4	65	1.93	1.78
132	810	C	10H	6	35	86.25	67	65.9	41.9	72.2	2.03	1.91
132	810	C	10H	6	113	87.03	66.7	65	39.9	66.3	2.01	1.83
132	810	C	10H	7	58	87.98	64.2	62.9	38.4	62.4	1.79	1.68
132	810	C	11H	1	39	88.29	64.8	63	38.7	63.2	1.84	1.68
132	810	C	11H	1	132	89.22	64.7	62.3	38.3	62.2	1.83	1.63
132	810	C	11H	2	133	90.73	63.4	61	36.8	58.1	1.73	1.55
132	810	C	11H	3	133	92.23	67.4	64.7	40.8	68.9	2.07	1.81
132	810	C	11H	4	134	93.74	65.9	63.1	39	63.8	1.93	1.69
132	810	C	11H	6	38	95.78	64.6	62.3	38	61.3	1.83	1.63
132	810	C	11H	7	14	97.04	62.5	60.6	36.7	58.1	1.67	1.52
132	810	C	11H	7	60	97.5	62.8	60.6	36.6	57.8	1.69	1.52
132	810	C	12H	1	30	97.7	65.6	64	39.5	65.3	1.9	1.76
132	810	C	12H	1	133	98.73	65.9	63.8	39.8	66	1.93	1.74
132	810	C	12H	2	134	100.24	55.4	53.9	30.4	43.7	1.24	1.16
132	810	C	12H	3	134	101.74	54.3	53.5	29.9	42.7	1.19	1.14
132	810	C	12H	5	40	103.8	49	50.8	26.7	36.5	.96	1.02
132	810	C	12H	6	102	105.92	54.2	53.6	29.6	42.1	1.19	1.14
132	810	C	13H	1	90	107.8	55.7	54.7	31	45	1.26	1.2
132	810	C	13H	2	90	109.3	59.5	58.8	34.4	52.4	1.47	1.41
132	810	C	13H	2	120	109.6	61.9	61.1	36.5	57.5	1.63	1.55
132	810	C	13H	3	130	111.2	59.9	58.5	34	51.5	1.49	1.39
132	810	C	13H	4	90	112.3	60.6	59.6	35.1	54	1.54	1.46
132	810	C	13H	5	35	113.25	57	55.7	31.9	46.8	1.33	1.24
132	810	C	13H	5	110	114	60.1	58.2	33.9	51.3	1.5	1.38
132	810	C	13H	6	59	114.99	60.6	59.9	35.2	54.2	1.54	1.48
132	810	C	14H	1	128	117.68	63.7	62.9	37.8	60.7	1.75	1.68
132	810	C	14H	2	79	118.69	63	62.4	38	61.3	1.7	1.64
132	810	C	14H	3	65	120.05	57.2	56.6	32	47	1.34	1.29

Table 7 (continued).

LEG	SITE	H	CORE	S	TOP	MBSE	POR1	POR2	WC/W	WC/D	VR1	VR2
132	810	C	14H	3	88	120.28	4.8	5.2	1.9	1.9	.05	.05
132	810	C	14H	5	116	123.56	60	59.7	35.1	54	1.5	1.47
132	810	C	14H	6	35	124.25	61	59.9	35.6	55.3	1.57	1.48
132	810	C	14H	6	99	124.89	60.9	58.9	34.1	51.7	1.56	1.42
132	810	C	15H	1	50	126.4	61.1	60.1	35.6	55.3	1.57	1.49
132	810	C	15H	1	100	126.9	58.8	58.4	33.8	51	1.43	1.39
132	810	C	15H	2	100	128.4	69.7	66.9	42.2	72.9	2.3	1.99
132	810	C	15H	4	35	130.75	71.9	70	46.4	86.6	2.55	2.3
132	810	C	15H	5	20	132.1	74.2	72.3	48.8	95.3	2.88	2.57
132	810	C	16X	1	1	127.11	5.2	5	2	2	.05	.05
132	810	C	16X	1	131	128.41	73.7	66.4	41.4	70.5	2.8	1.95
132	810	C	16X	2	97	129.57	61.4	60.6	35.8	55.8	1.59	1.52

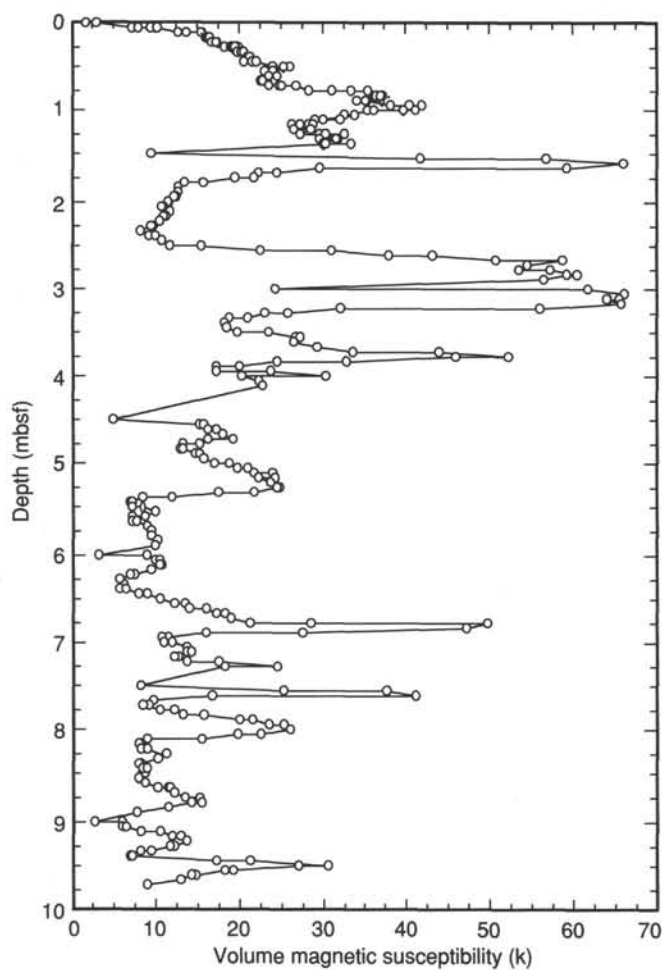


Figure 24. Plot of volume magnetic susceptibility (k) vs. depth from 0 to 10 mbsf for Hole 810A.

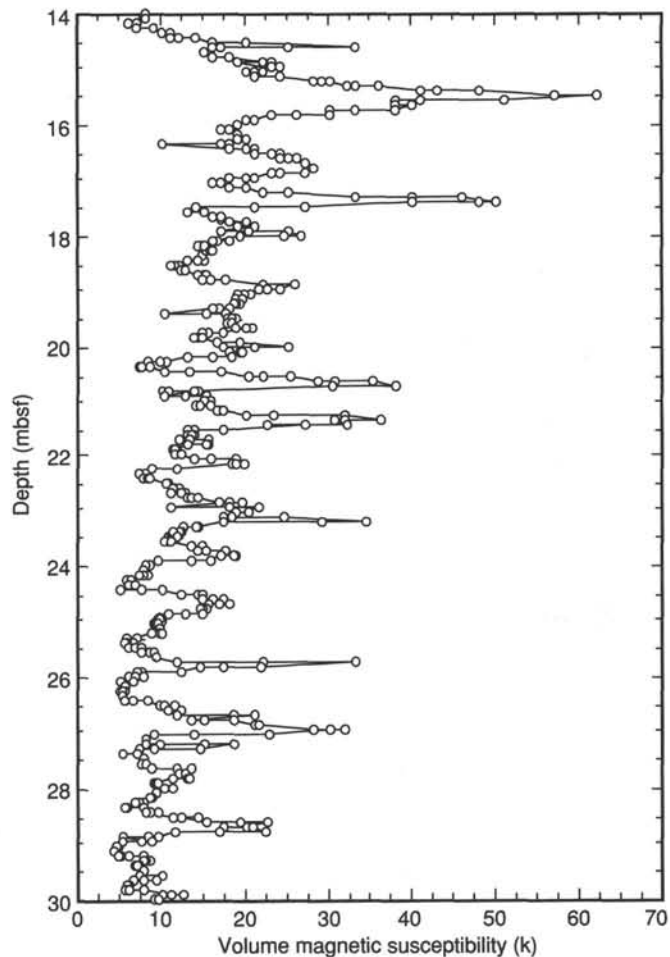


Figure 25. Plot of volume magnetic susceptibility (k) vs. depth from 14 to 30 mbsf for Hole 810C. Note the alternating pattern of peaks and troughs with approximately 0.5 m spacing in susceptibility data.

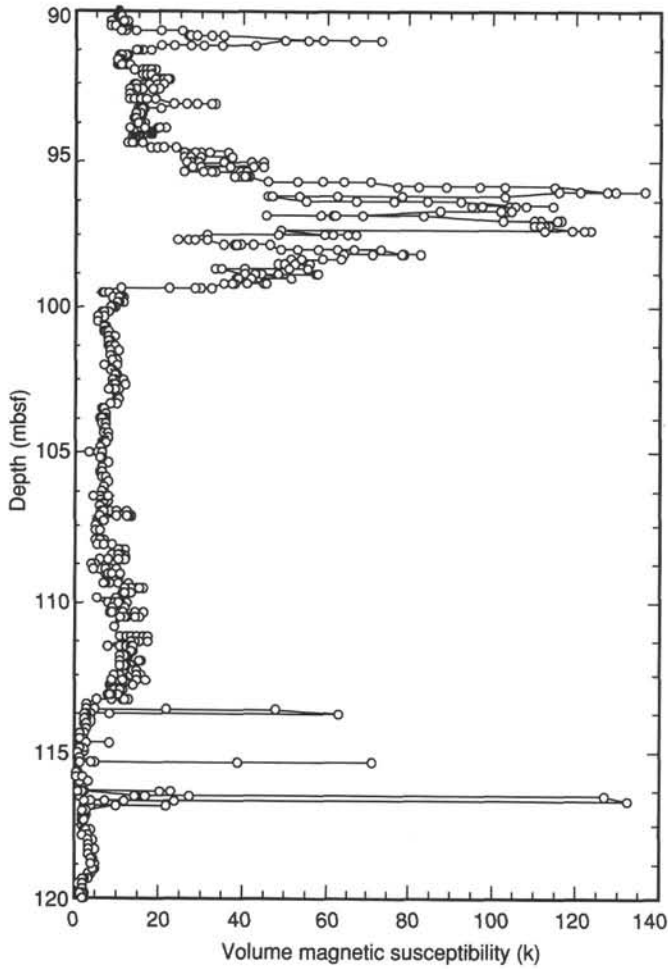


Figure 26. Plot of volume magnetic susceptibility (k) vs. depth from 90 to 120 mbsf for Hole 810C. Note the large decrease in susceptibility below 99.5 mbsf.

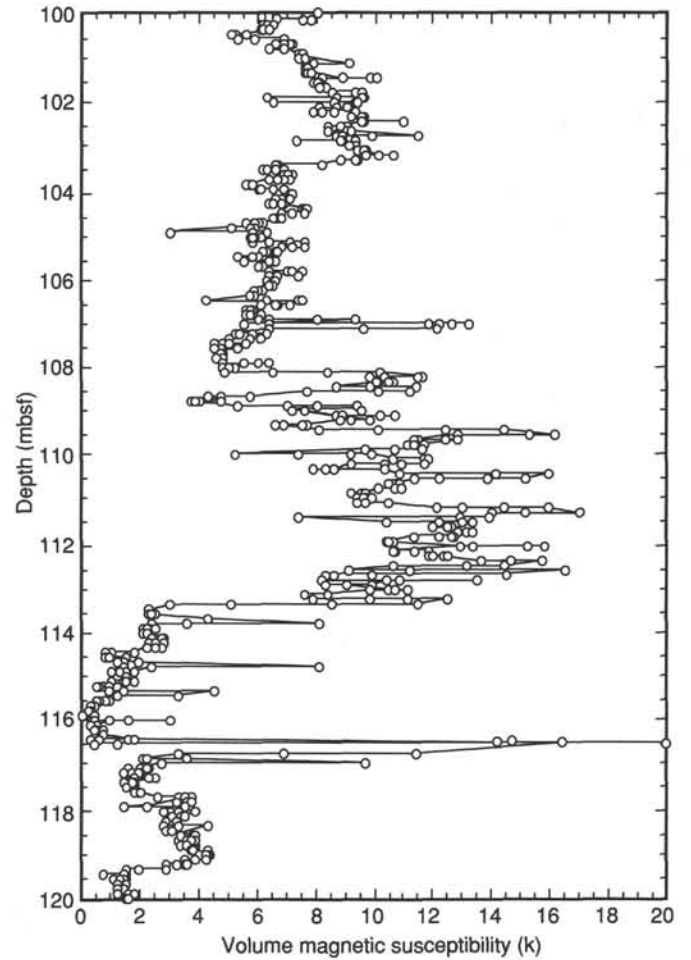


Figure 27. Plot of volume magnetic susceptibility (k) vs. depth from 100 to 120 mbsf for Hole 810C. Note scale difference compared with Figure 26. Decreases in susceptibility at approximately 103 and 113.3 mbsf represent possible hiatuses. The variable susceptibility values between 108 and 113.3 mbsf represent a zone of sediment reworking or slumping.

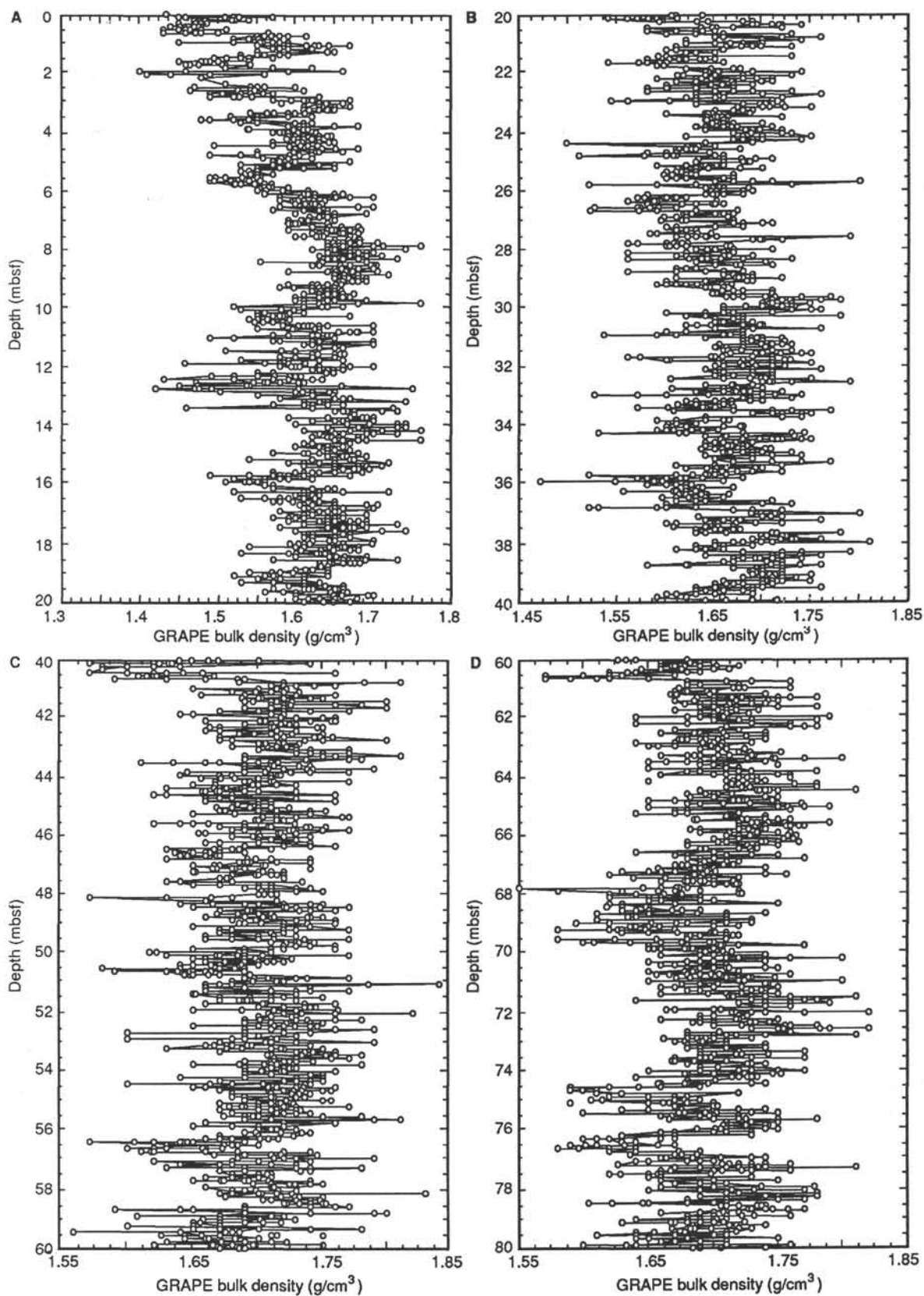


Figure 28. Plots of GRAPE bulk density (g/cm^3) vs. depth (mbsf) for 20 m intervals downhole at Hole 810C. A. 0–20 mbsf. B. 20–40 mbsf. C. 40–60 mbsf. D. 60–80 mbsf. E. 80–100 mbsf. F. 100–120 mbsf. G. 120–140 mbsf.

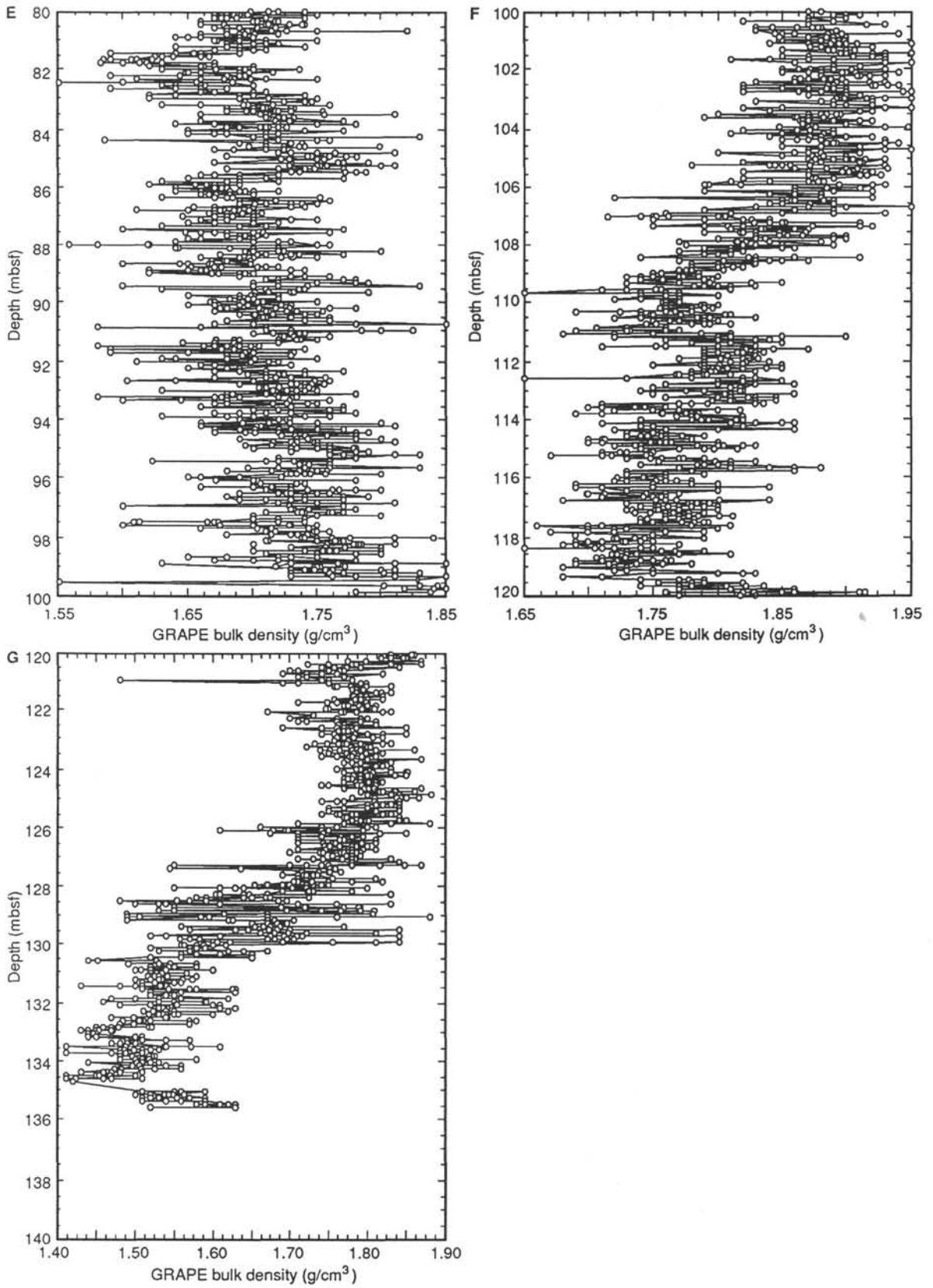


Figure 28 (continued).

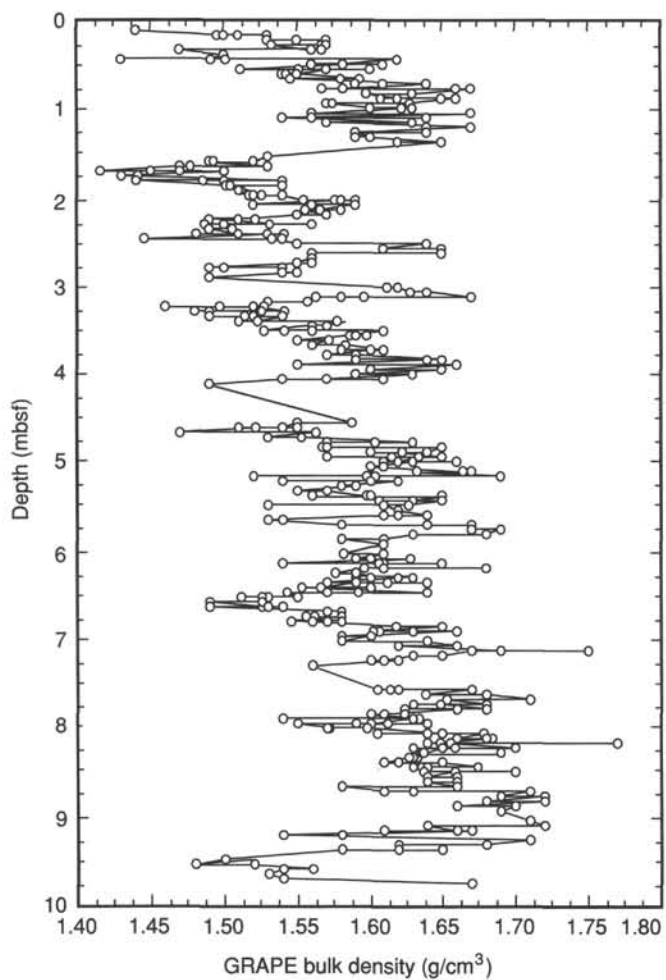


Figure 29. Plot of GRAPE bulk density (g/cm^3) vs. depth (mbsf) for Hole 810A. Note depth scale difference compared with Figure 28A.

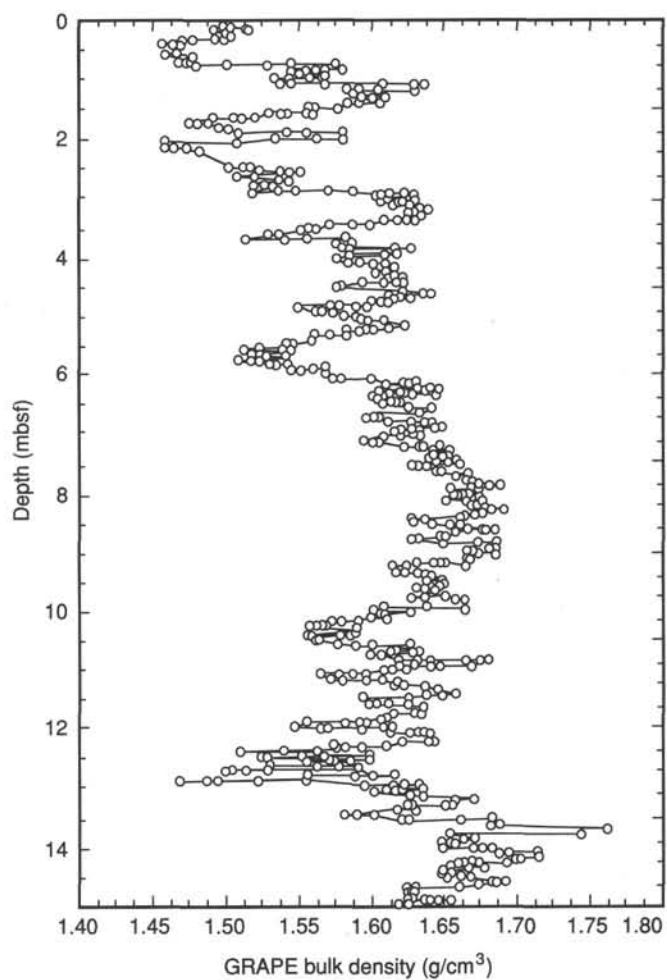


Figure 30. Plot of GRAPE bulk density (g/cm^3) vs. depth from the mud line to 15 mbsf for Hole 810C.

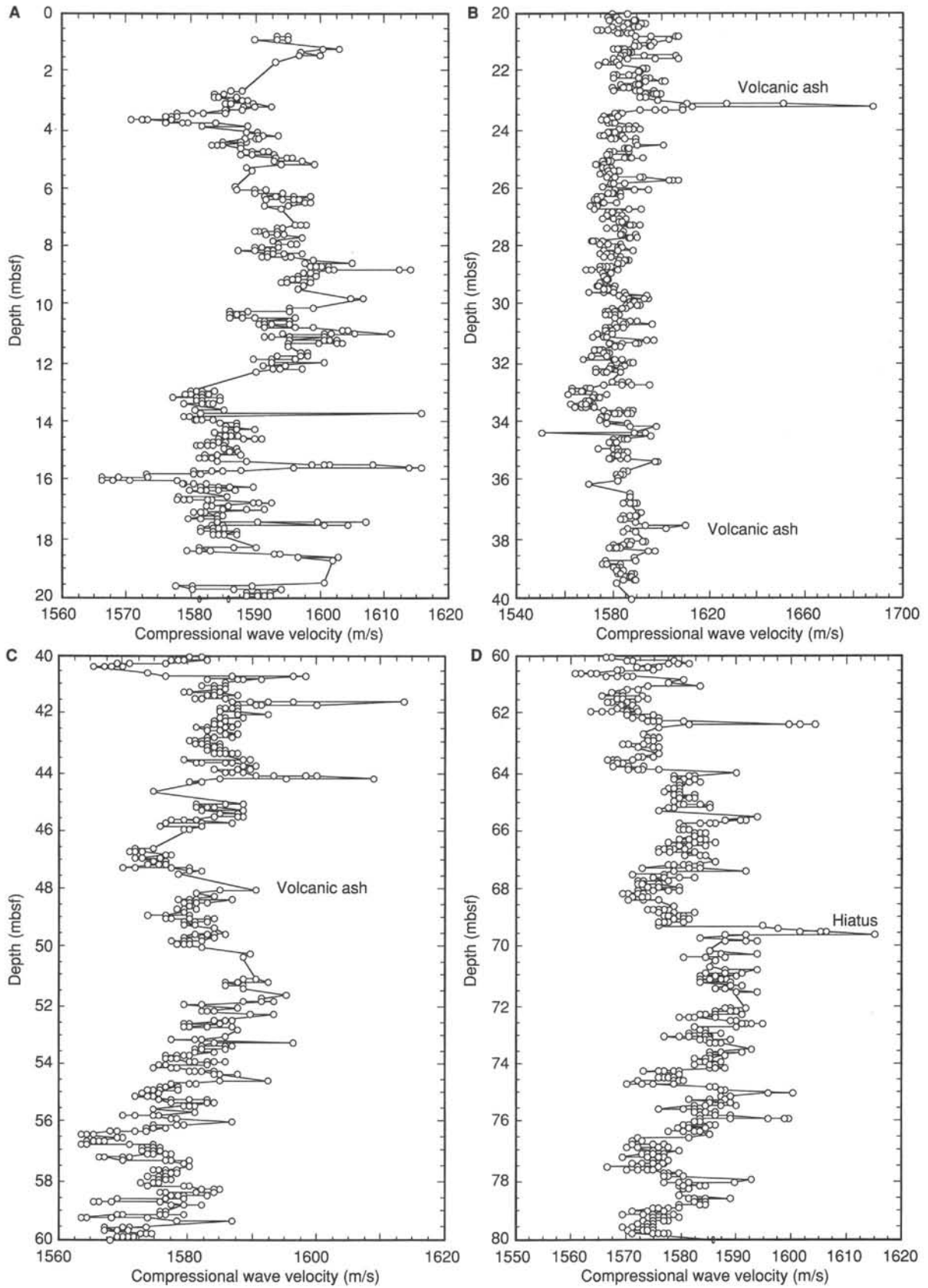


Figure 31. Plots of compressional wave velocity (m/s), measured with the PWL, vs. depth (mbsf) for 20 m intervals at Hole 810C. A. 0–20 mbsf. B. 20–40 mbsf. C. 40–60 mbsf. D. 60–80 mbsf. E. 80–100 mbsf. F. 100–120 mbsf. G. 120–140 mbsf. The locations of identified ash layers, hiatuses, and chert are noted in the appropriate plots. Velocities at the base of the hole range from 1640 to 1680 m/s.

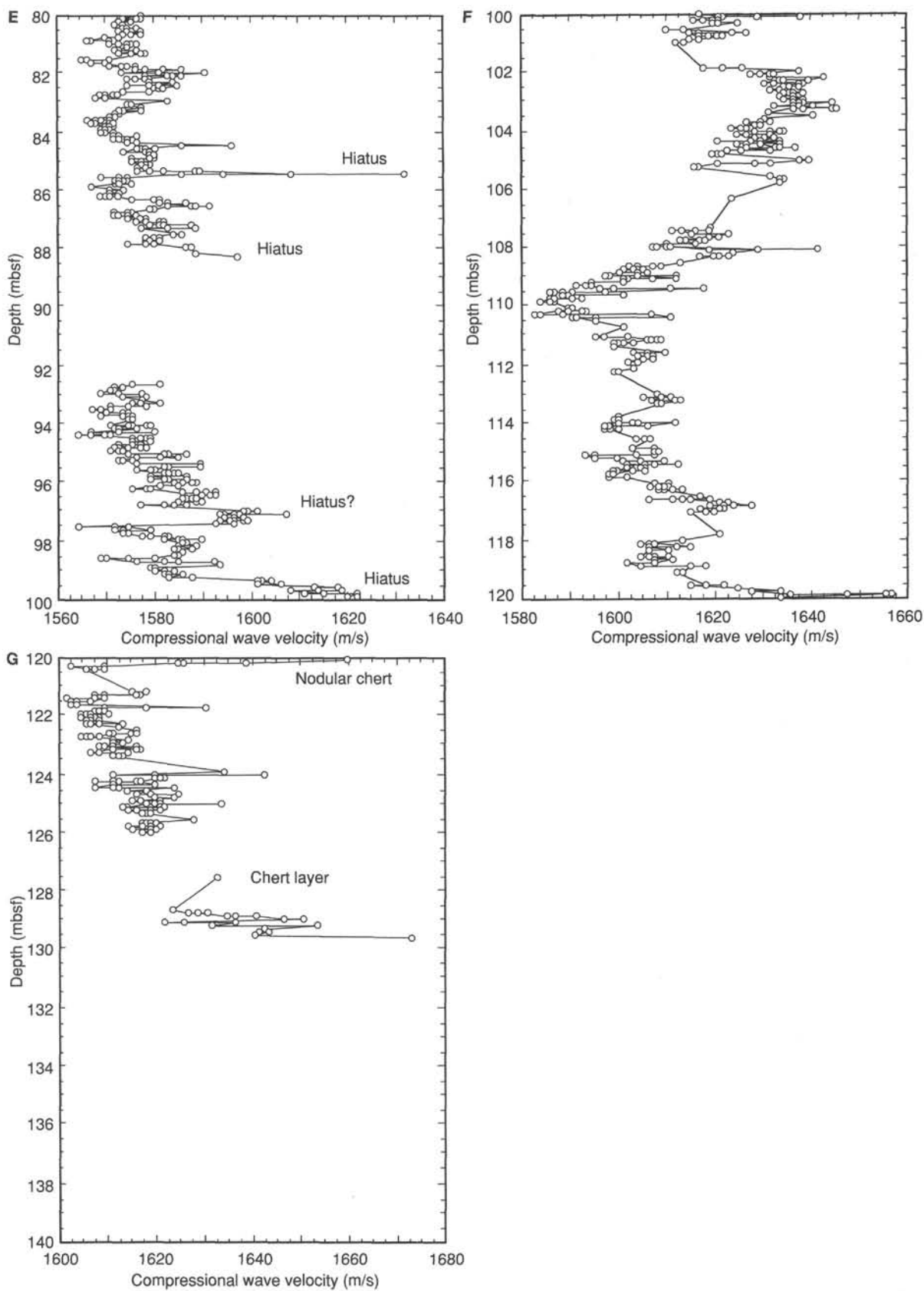


Figure 31 (continued).